ELSEVIER

Chemical Geology 206 (2004) 259–288

CHEMICAL GEOLOGY
INCLUDING
ISOTOPE GEOSCIENCE

www.elsevier.com/locate/chemgeo

High-resolution geochemistry and sequence stratigraphy of the Hushpuckney Shale (Swope Formation, eastern Kansas): implications for climato-environmental dynamics of the Late Pennsylvanian Midcontinent Seaway

Thomas J. Algeo[a,*], Lorenz Schwark[b], James C. Hower[c,d]

[a] *Department of Geology, University of Cincinnati, Cincinnati, OH 45221-0013, USA*
[b] *Geologisches Institut, Universität zu Köln, Zülpicher Str. 49a, D-50674 Köln, Germany*
[c] *Center for Applied Energy Research, 2540 Research Park Drive, Lexington, KY 40511-8410, USA*
[d] *Department of Geological Sciences, University of Kentucky, Lexington, KY 40506-0059, USA*

Accepted 23 December 2003

Abstract

The Hushpuckney Shale Member of the Swope Formation (Missourian Stage, eastern Kansas) is the core shale of a Kansas-type cyclothem, formed during the late transgressive to early regressive phases of a Late Pennsylvanian glacio-eustatic cycle. Coeval high-frequency climato-environmental dynamics of the Midcontinent Seaway are preserved in the KGS Orville Edmonds No. 1A study core as centimeter-scale variation in major components (organic carbon, authigenic sulfides and phosphate, detrital siliciclastics), organic macerals, trace-element redox proxies (Mo, U, V, Zn), and ichnofabric features. Benthic O_2 levels declined sharply from the base of the black shale (0 cm), went sulfidic at ~4 cm, and reached a redox minimum at ~21 cm; above this level, redox potential gradually rose, fluctuating between sulfidic and nonsulfidic conditions from ~35 cm to the black shale/gray shale contact at 52 cm. Onset of dysoxic conditions at that contact allowed establishment of a benthic community of soft-bodied organisms comprised of deep-tiered tracemakers tolerant of low-O_2 conditions (*Trichichnus*), and shallow-tiered tracemakers favoring "soupground" (*Helminthopsis*) or "firmground" substrates (the *Zoophycos–Phycosiphon–Schaubcylindrichnus–Planolites* association). Most geochemical records exhibit a "low-order" cycle spanning the full 52 cm thickness of the black shale submember, reflecting a dominant glacio-eustatic control. The base and top of the black shale submember record lateral migration of the pycnocline across the Midcontinent Shelf during the transgressive and regressive phases, respectively. The maximum flooding surface (MFS) is at ~17–23 cm, an interval containing the euxinic peak and characterized by high concentrations of illite (representing a cratonic siliciclastic flux) and terrestrial organic macerals, the product of transient increases in humidity, weathering rates, and the export of coal-swamp vegetation associated with the interglacial highstand of the Swope cyclothem. Although a transgressive "surface of maximum starvation" (SMS) cannot be confidently identified, a phosphate-rich "regressive condensation surface" at ~28–34 cm records pycnoclinal weakening due to increased aridity associated with renewed southern hemisphere icesheet growth; a correlative shift in dominance from terrestrial- to marine-derived organic macerals reflects increased upwelling of nutrient-rich deepwaters and enhanced primary productivity. Penecontemporaneous paleogeographic and -climatic factors (e.g., semirestricted circulation, monsoonal precipitation) predisposed the Midcontinent Seaway toward sensitivity to high-frequency climato-

* Corresponding author. Tel.: +1-513-556-4195; fax: +1-513-556-6931.
E-mail addresses: Thomas.Algeo@uc.edu (T.J. Algeo), lorenz.schwark@uni-koeln.de (L. Schwark), hower1a@caer.uky.edu (J.C. Hower).

doi:10.1016/j.chemgeo.2003.12.028

environmental fluctuations, which are preserved as 2- to 7-cm-thick cycles in the study core. The 52-cm-thick black shale submember contains ~12 such "high-order" cycles, which have an estimated average duration of ~2 to 9 kyr, implying a sub-Milankovitch-band (i.e., millennial scale) climatic control. The results of this study are relevant to the sequence stratigraphic interpretation of Kansas-type cyclothems, the dynamics of Gondwanan Ice Age glacio-eustatic cycles, and the development of boundary conditions for Late Pennsylvanian paleoclimate models.

Keywords: Black shales; Organic carbon; Redox facies; Trace elements; Cyclothems; Eustasy; Paleoclimate

1. Introduction

Although the sequence stratigraphy of Upper Pennsylvanian Kansas-type cyclothems has been well-documented in recent years (e.g., Watney et al., 1989, 1995; Heckel, 1991; Bisnett and Heckel, 1996; Felton and Heckel, 1996; Miller et al., 1996; Miller and West, 1998; Mazzullo, 1998; Olszewski and Patzkowsky, 2003), core black shales have been the subject of only a handful of high-resolution geochemical and petrographic studies (e.g., Wenger and Baker, 1986; Hatch and Leventhal, 1992; Genger and Sethi, 1998; Cruse and Lyons, 2000), none of which has been sufficiently detailed to permit development of an internal sequence stratigraphic framework. In this study, centimeter-scale analysis of the Hushpuckney Shale Member of the Swope Formation documented a number of distinctive horizons having probable sequence stratigraphic and climato-environmental significance, some of which exhibit unusual, and previously unreported, geochemical and petrographic characteristics. For example, the horizon identified as the maximum flooding surface (MFS) is associated with a large illite anomaly and peak concentrations of terrestrial-derived organic macerals and redox-sensitive trace elements (TEs); these features suggest increased humidity and chemical weathering, large-scale export of coal-swamp vegetation, and pycnoclinal strengthening and benthic oxygen depletion during the Swope cyclothem highstand. A "regressive condensation surface" above the MFS is associated with a high density of authigenic phosphate granule layers, a shift in dominance from terrestrial- to marine-derived organic macerals, and a sharp decrease in the concentrations of redox-sensitive trace elements; these features suggest climatic drying and coal-swamp destruction, greater vertical mixing and benthic oxygenation, and enhanced upwelling and primary productivity. These horizons and others provide the basis for development of a detailed sequence stratigraphic framework within the Hushpuckney Shale, from which eustatic and climato-environmental dynamics of the Late Pennsylvanian Midcontinent Seaway can be evaluated. In all, the present study suggests a more complex interplay of eustatic and climatic factors during the formation of core black shales than heretofore recognized.

GCMs and other climate models have been used to investigate Permo-Carboniferous paleoclimates (e.g., Crowley et al., 1989, 1996; Parrish, 1993). These studies suggest that Late Pennsylvanian Midcontinent North America had a subtropical climate with moderate precipitation of strongly seasonal (monsoonal) character, and that paleogeographic factors contributed not only to seasonal but also to long-period climatic cyclicity through modulation of atmospheric circulation patterns and monsoonal intensity. Potential synergies between paleoclimate and sequence stratigraphic research on the Late Pennsylvanian exist; the latter is essential for documenting the patterns of long-period climatic cyclicity predicted by the former and can be useful in setting boundary conditions for paleoclimate models. Core black shales are especially well-suited for integrated sequence stratigraphic–paleoclimatic analyses because they were deposited (1) under anoxic conditions, in which millimeter-thick laminae provide a high-resolution record of temporal events, (2) in a climatically sensitive marine environment that responded readily to small perturbations, (3) during interglacial epochs, which were characterized by strong climate variation, and (4) over wide geographic areas, allowing analysis of regional dynamics of the Midcontinent Seaway and the Late Pennsylvanian climate system.

2. Geologic setting

Missourian Stage strata are exposed in a 500-km-long belt extending from Oklahoma to Iowa, representing a northeast–southwest transect across the Late Pennsylvanian Midcontinent Shelf (n.b., all directional references represent paleo-orientations). The study core, located in northeastern Kansas, represents a mid-shelf setting equivalent to the "open marine facies" of Heckel (1977) (Fig. 1a). The low topographic relief of the shelf resulted in lateral shifts of the paleoshoreline over distances of hundreds of kilometers, with northward transgressions flooding the southern margins of the low-lying Laurentian craton (Fig. 2; Heckel, 1986; Boardman and Heckel, 1989; Watney et al., 1989, 1995; Joeckel, 1994, 1999). The southern margin of the shelf was approximately coincident with the boundary between the phylloid algal mound and terrigenous detrital facies belts of Heckel (1977) in southeastern Kansas. To the south and southwest, the Midcontinent Shelf was separated from the active Ouachita–Marathon uplifts by the narrow but intermittently deep Anadarko and Arkoma foreland basins (Arbenz, 1989). At distances of >1000 km, the Ancestral Rocky Mountains rose to the west and the Alleghenian Orogen to the east (Ettensohn, 1992; Cullers, 1994). The Midcontinent Shelf was thus isolated from sources of proximally derived, coarse-grained siliciclastics, and the fine-grained material (i.e., clays) that it received may have been polysourced.

During the Late Pennsylvanian, Midcontinent North America was located at 5–10°N latitude (Fig. 2; Heckel, 1977; Scotese, 1994). The region had a warm climate (10–25 °C), limited seasonal temperature range (<15 °C), and moderate annual precipitation (<73 cm yr^{-1}; Crowley et al., 1989, 1996; Parrish, 1993). Climatic conditions trended toward greater aridity during the Middle to Late Pennsylvanian as North America drifted northward out of the humid tropical belt (Schutter and Heckel, 1985; Cecil, 1990; Scotese, 1994). This led to more seasonal precipitation, consistent with development of vertisols and aridisols in the Midcontinent during the Late Pennsylvanian (Schutter and Heckel, 1985). Strongly seasonal (monsoonal) precipitation was favored by (1)

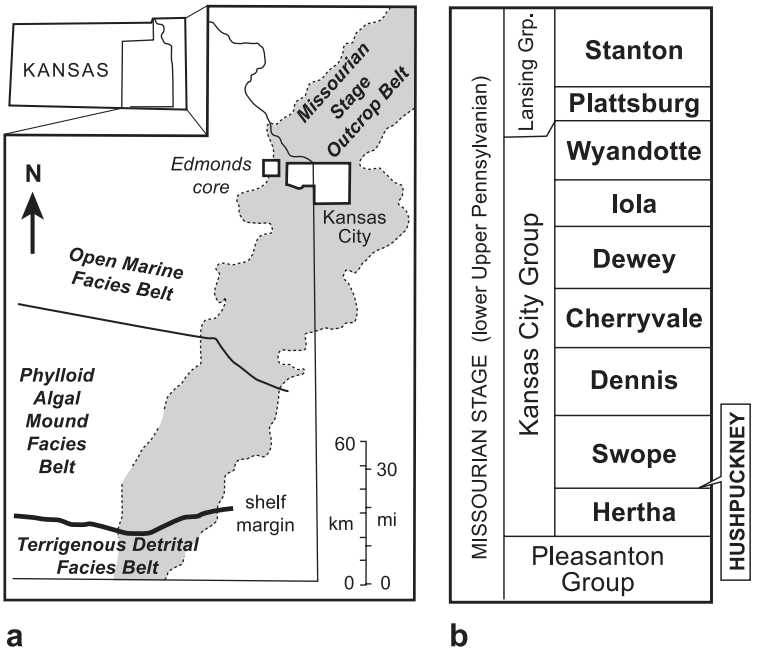

Fig. 1. (a) Location of the Kansas Geological Survey Orville Edmonds No. 1A core. Missourian Stage outcrop and facies belts from Heckel (1977). (b) Missourian Stage stratigraphy of the Midcontinent Shelf. The Hushpuckney Shale is the core shale member of the Swope Formation (or cyclothem) of the Kansas City Group.

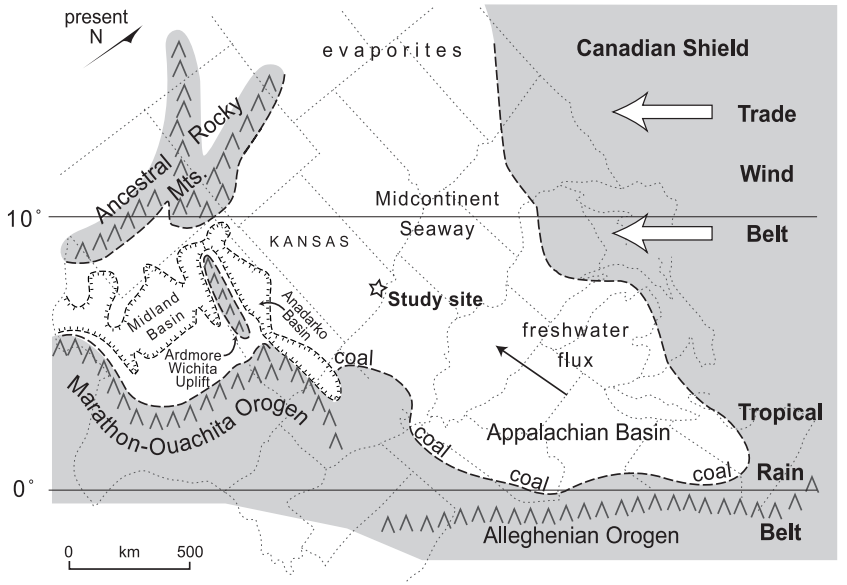

Fig. 2. Paleogeography of Late Pennsylvanian North America (modified from Heckel, 1977, 1991). The study site was located in the middle of the Midcontinent Seaway, hundreds of kilometers distant from shelf margins and paleoshorelines (i.e., at maximum transgression, as shown here).

large annual changes in air pressure over Pangea, and (2) a source of moisture and latent energy in the large Tethyan oceanic embayment to the east (Parrish, 1993; Crowley et al., 1996). Proximity to the paleo-ITCZ (Intertropical Convergence Zone) enhanced the potential for temporal changes in atmospheric circulation patterns (Parrish, 1993). These factors contributed not only to annual but also to long-period climatic cyclicity through modulation of the seasonality and intensity of monsoonal precipitation by, e.g., orbital forcing (Cecil, 1990; Soreghan et al., 2002).

The Gondwanan Ice Age lasted ~100 Myr, peaking during the Late Mississippian–Early Permian as poleward oceanic heat transport intensified in response to tectonic closing of the paleo-Tethyan Seaway (Crowell, 1978, 1999; Veevers and Powell, 1987; Frakes et al., 1994; Saltzman, 2003). At maximum development, Gondwanan icesheets were comparable in size to those of the Late Pleistocene, covering $\sim 24\times10^6$ km^2 and causing global sea-level changes of ~60–120 m (Crowley and Baum, 1991; Soreghan and Giles, 1999). Glacio-eustatic fluctuations driven by waning and waxing of continental icesheets produced transgressive–regressive packages known as cyclothems that, at relatively coarse scales ("third-order" and "fourth-order"), are regionally or globally correlatable (Ross and Ross, 1985; Connolly and Stanton, 1992; Youle et al., 1994). In the study area (eastern Kansas), the Missourian succession consists mainly of interstratified marine shales and limestones deposited in 10- to 50-m-thick "Kansas-type" cyclothems (Fig. 1b; Heckel, 1977). Core shales such as the Hushpuckney Shale Member of the Swope Formation (Kansas City Group, Missourian Stage) represent late transgressive to early regressive phases of glacio-eustatic cycles of the Gondwanan Ice Age (Heckel, 1994).

During interglacial highstands, the Midcontinent Seaway was a stratified water mass, causing benthic O_2 depletion that facilitated accumulation of large quantities of sedimentary organic carbon. Stratification may have been stronger in proximal portions of the seaway (to the north and east) owing to formation of a halocline associated with strong freshwater runoff from the Alleghenian Mountains; weaker stratification in distal areas (to the south and west) was due to a thermocline (Heckel, 1991; Hatch and Leventhal, 1992; Hoffman et al., 1998). Stratification of the Midcontinent Seaway may have been favored by paleogeographic and climatic factors (Fig. 2): (1)

semi-enclosure by landmasses, reducing exchange with the open ocean and increasing runoff volume per unit area; (2) strong precipitation and runoff owing to proximity to the humid tropical belt and the paleo-ITCZ (Intertropical Convergence Zone; Parrish, 1993; Scotese, 1994); and (3) more humid conditions during interglacials than during associated glacial stages (Cecil, 1990; Rankey, 1997; West et al., 1997; Soreghan et al., 2002; Olszewski and Patzkowsky, 2003). The core shales of Kansas-type cyclothems are generally regarded as representing a sediment-starved, low-oxygen environment based on their fine grain size, high concentrations of organic carbon and authigenic phosphate, enrichment in many redox-sensitive trace elements, absence of biota other than rare pelagic organisms, and ^{34}S-depletion of authigenic Fe-sulfides (Heckel, 1977, 1991; Coveney and Shaffer, 1988; Schultz and Coveney, 1992; Hatch and Leventhal, 1992; Hoffman et al., 1998).

3. Methods

The Hushpuckney Shale was studied in the Kansas Geological Survey (KGS) Orville Edmonds No. 1A core, from Leavenworth County, Kansas (Sec. 35, Twp. 9S, Range 22E; Fig. 1a). The study core was minutely described and analyzed using X-radiographic, petrographic, and geochemical techniques. X-radiography was used (1) to examine very fine (subcentimeter) scale compositional variation in the study core, (2) to visually determine the distribution of authigenic phosphate nodules and certain ichnofabric features, and (3) to select sample intervals of relatively uniform composition for geochemical analysis. Gray-scale variation in X-radiographs records density differences that are due to compositional variation: organic matter content (as proxied by TOC) is the dominant control on gray-scale variance (Algeo and Maynard, 1997). X-radiograph images were produced at the University of Cincinnati using a tungsten-source Hewlett Packard Faxitron (model 43804N) and a custom-built core stage (Algeo et al., 1994).

Petrographic analysis entailed (1) low-magnification binocular microscopy to study ichnofabric features, and (2) high-magnification monocular microscopy to study organic macerals. The ichnofabric of the study core was described in reference to matrix and burrow color, bioturbation intensity, and burrow system features (e.g., dimensions, spreiten, linings, wall morphology, and cross-cutting relationships). Matrix (i.e., sediment outside burrows and distinct from burrow fill) and burrow colors were estimated using a Munsell color chart. Bioturbation intensity was assessed using the ichnofabric index (ii) scale of Droser and Bottjer (1993), ranging from ii1 (undisturbed laminae) to ii6 (fabric completely homogenized by burrowing). Burrow dimensions (e.g., maximum diameter, maximum penetration depth) were measured according to procedures of Savrda and Bottjer (1991). Taxonomic classification of ichnogenera followed Ekdale et al. (1984), Ekdale and Mason (1988), Bromley (1996), and Savrda et al. (2001). For organic petrographic analysis, core sections ~10 cm in length were epoxied and marked off in increments corresponding to the individual centimeter-thick samples taken for geochemical analysis. The polished slabs were examined at high magnification under reflected white and violet–UV fluorescent light. Organic macerals and other components were quantified by point count with a minimum of 300 observations per sample interval collected using a 0.3×0.3 mm grid. Macerals were classified based on shape, structure, reflectance, and UV character using standard references (e.g., Falcon and Snyman, 1986; Hutton, 1987; Tyson, 1995).

A total of 51 samples were collected for geochemical analysis: 42 samples from the black shale submember, averaging 1.2 cm in thickness, and 9 samples from the overlying gray shale submember. Samples were ground in an agate ball mill and refrigerated prior to analysis. Trace-element concentrations were determined by XRF using a wavelength-dispersive Rigaku 3040 XRF spectrometer at the University of Cincinnati. Samples were calibrated with both USGS (SDO-1, Sco-1, SGR-1) and internal black shale standards (analyzed by XRAL Incorporated). Analytical precision based on replicate analyses was better than ±5% for the major and trace elements reported here. Detection limits for trace elements were 2 ppm for Mo, 5 ppm for Zn, and 10 ppm for U and V. Trace-element concentrations are reported normalized to Al (units of 10^{-4}) to correct for variable dilution by organic matter and authigenic minerals (e.g., Arthur et al., 1990; Morford et al., 2001). A LECO CS-244 analyzer at Indiana University was used to determine total carbon

(TC), total organic carbon (TOC; by leaching with 10% HCl), and total sulfur (TS). Samples for LECO analysis were calibrated with internal laboratory standards; analytical precision (2σ) based on replicate analyses was ±2.0% and ±7.6% of measured values for C and S, respectively. Pyrolysis on total rock samples was performed using a ROCK EVAL II-PLUS analyzer (Vinci Technologies) at the University of Köln, Germany, following standardized procedures reported by Espitalié et al. (1977, 1985) and Bordenave et al. (1993). Geochemical and petrographic data are available from the first author upon request.

4. Results

4.1. General character

The Hushpuckney Shale Member of the Swope Formation in the KGS Orville Edmonds No. 1A study core consists of a 52-cm-thick black shale submember overlain by a ~36-cm-thick gray shale submember (Fig. 3). The black shale is nonfossiliferous, laminated to weakly burrowed, and moderately to highly phosphatic. It contains abundant, well-preserved organic matter (e.g., TOC=2.5–40 wt.%; hydrogen index [HI]=290–410) consisting of vitrinitic, inertinitic, exinitic, and bituminitic macerals (Figs. 4–5). The overlying gray shale is nonfossiliferous, has a homogenized fabric exhibiting discrete traces, and contains little or no phosphate. It contains limited quantities of poorly preserved organic matter (e.g., TOC<2.5 wt.%; HI=200–290) consisting almost exclusively of exinitic and bituminitic macerals (Figs. 4–5). Above ~85 cm, the gray shale is completely homogenized (i.e., without visible macroburrows) and transitions over several centimeters into an argillaceous fossiliferous wackestone (base of the Bethany Falls Limestone Member of the Swope Formation). We analyzed the Hushpuckney Shale from the base of the black shale submember (0 cm) to the top of the discretely burrowed zone of the gray shale submember (~85 cm) in the study core.

4.2. Stratification

The Hushpuckney Shale is underlain by the Middle Creek Limestone Member of the Swope Formation, which is predominantly a phylloid algal wackestone consisting of large, unbroken to partially fragmented algal fronds. The uppermost few centimeters of the limestone are discolored to grayish tones and show evidence of dissolution along closely spaced microstylolites, probably related to an increase in clay content or organic matter. The contact itself is slightly irregular in relief and penetrated by burrows with indistinct margins containing small amounts of piped organic-rich mud to a depth of ~1–2 cm below the contact. Above the contact is a 1-cm-thick layer of heavily corroded, fine carbonate skeletal debris, mainly consisting of small bivalves (?). It is unclear whether the dissolution features at the top of the Middle Creek Limestone represent syndepositional corrosion, e.g., associated with sediment starvation, or diagenetic corrosion, e.g., associated with downward flux of acidic porewaters from the overlying black shale.

The black shale submember is finely laminated throughout and exhibits few macroscopic features other than scores of thin authigenic phosphate granule layers (Fig. 3b). Individual layers are mostly <2 mm thick, laminar (or occasionally lens-shaped), and grouped in closely spaced sets from one to a few centimeters in thickness. Phosphate granule layers are present from ~4 to 47 cm (i.e., through most of the black shale submember) but are most numerous and individually thickest in the interval from ~28 to 34 cm. Each layer consists of round or ellipsoidal particles that show faint concentric internal lamination; most are <1 mm in size, but larger particles (3–4 mm in diameter) are present in the granular layers at ~28–34 cm. There are no macroscopic (i.e., >1 cm diameter) authigenic phosphate nodules in the study core, such as those found in the Hushpuckney Shale further to the southwest (cf. Kidder et al., 1996; Algeo and Maynard, 1997). Evidence of current reworking is limited to a few lens-shaped phosphate granule layers, mostly located in the high-density interval at ~28–34 cm. That intraformational winnowing and erosion was limited is suggested by the fact that individual centimeter-thick layers within the black shale submember can be correlated laterally over distances of >100 km on the basis of distinctive patterns of compositional variation in X-radiographs (Algeo and Maynard, 1997, p. 136).

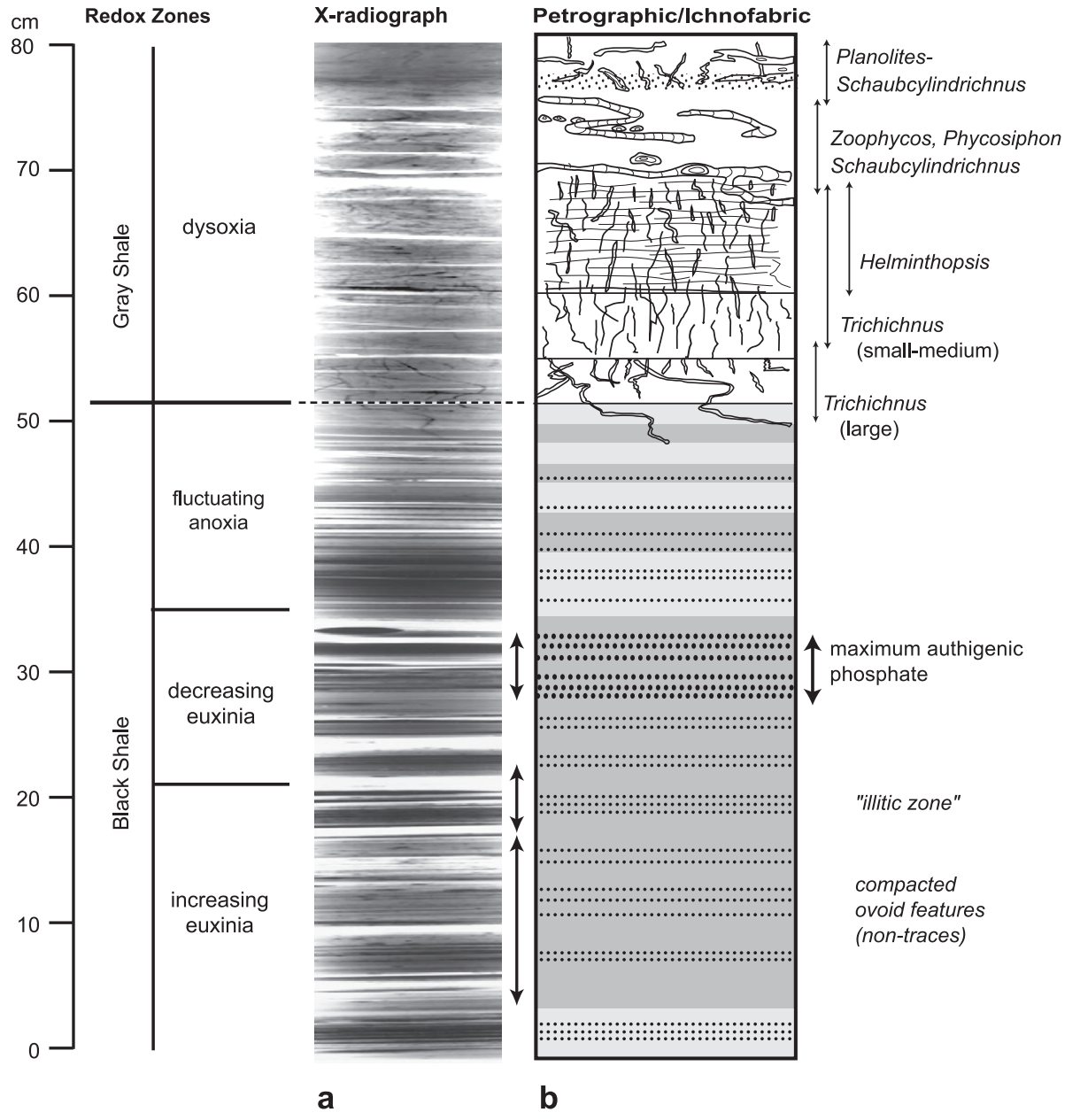

Fig. 3. Petrographic features of study core. (a) X-radiograph of split 2-in.-diameter core with ~5× horizontal exaggeration; denser features appear darker in this positive print. Note centimeter-scale compositional variation in the black shale submember, and lack thereof in the gray shale submember. Compacted ovoid features at ~4–17 cm are non-traces, e.g., fecal pellets or gelatinized remains of pelagic organisms; trace fossils are visible from ~50 cm upward. (b) Sketch of features visible in reflected light. The black shale submember contains numerous authigenic phosphate granule layers (dotted lines); the maximum concentration of layers and largest granule sizes are at ~28–34 cm. The gray shale submember contains numerous trace fossils grouped in discrete zones; ranges of important ichnogenera are shown at right (see text for discussion). Redox facies are shown by shaded backgrounds in (b): euxinia=dark gray, non-sulfidic anoxia=light gray, dysoxia=white (see Algeo and Maynard, 2004). For Figs. 3–4 and 6–8, the legend at left shows thickness in centimeters above the base of the black shale submember and general redox zones of the Hushpuckney Shale.

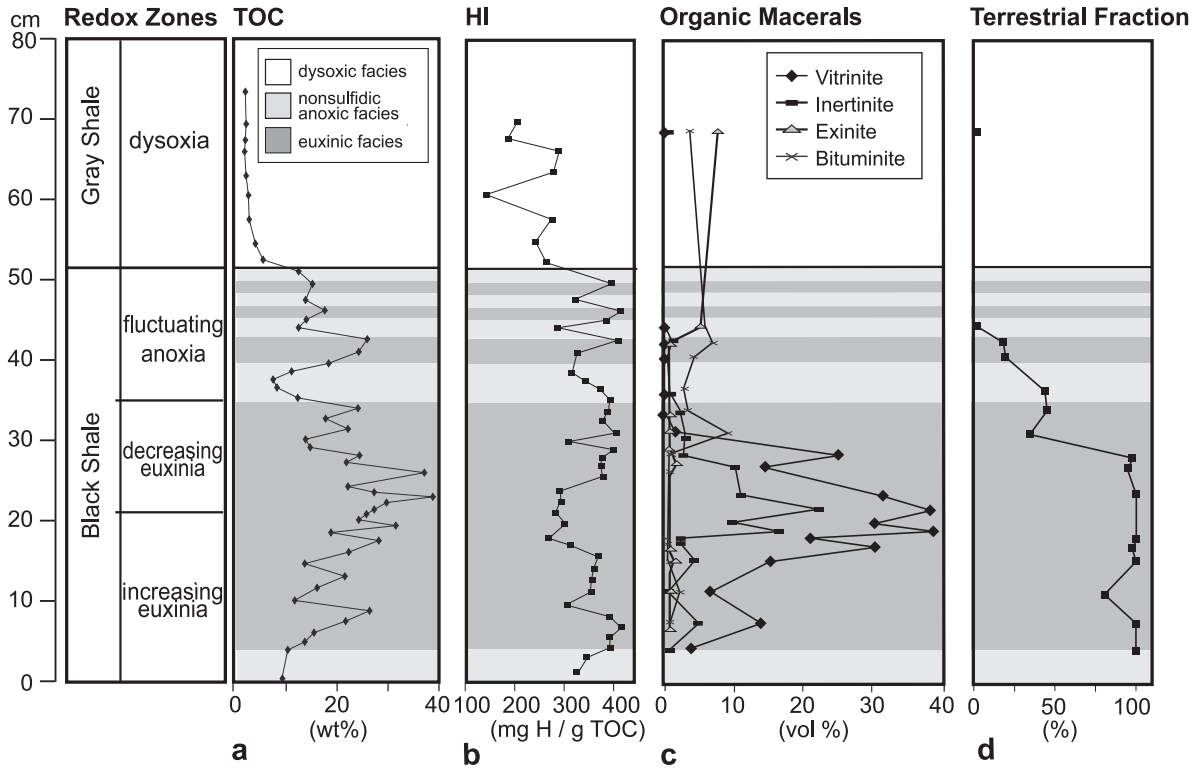

Fig. 4. Organic components of the study core. (a) Total organic carbon, or TOC (wt.%). (b) Hydrogen index, or HI (mg H g^{-1} TOC). (c) Organic macerals (vol.%; based on petrographic point-counts). (d) Terrigenous fraction, or F_{terr} (i.e., the ratio of vitrinite plus inertinite to total organic macerals; %).

The contact of the black shale with the overlying gray shale submember of the study core is at 52 cm. It is sharp, horizontal, and penetrated by *Trichichnus* burrows to a depth of ~3 cm (Fig. 3). Although this contact shows no features associated with syndepositional condensation or erosion, several horizons within the gray shale submember contain such evidence. At ~55 cm, the upper ends of many *Trichichnus* burrows are terminated at the same level, suggesting erosive truncation. At ~76 cm, a thin, weakly phosphatic layer contains small, angular, dark-colored clasts; the latter are either allochthonous or the remains of an in situ organic-rich horizon that was completely stripped away. The phosphatic layer exhibits reduced burrowing intensity as well as redirection of downward penetrating burrows, suggesting a firmground consistency at the time of deposition. These features are indicative of a slowdown or hiatus in sedimentation at this level.

4.3. Ichnofabric

Ichnofabric features provide information on gross patterns of benthic oxygenation within the study unit. A total lack of bioturbation (ii1; "ichnofabric index" of Droser and Bottjer, 1993) characterizes the black shale submember except for the uppermost ~3 cm (Fig. 3), suggesting that bottomwater conditions were sufficiently oxygen-depleted as to exclude benthic colonization. Largish (~0.5–1 cm horizontal diameter), dark (in X-radiographs, indicative of high density), vertically flattened "ovoid" features with indistinct margins are present in coplanar groups in the lower black shale (~4–17 cm), but these are not considered to be trace fossils because they show neither vertical penetration of laminae nor significant lateral extent, as would be expected with burrows. Rather, they are interpreted as compressed fecal pellets or gelatinized organic remains

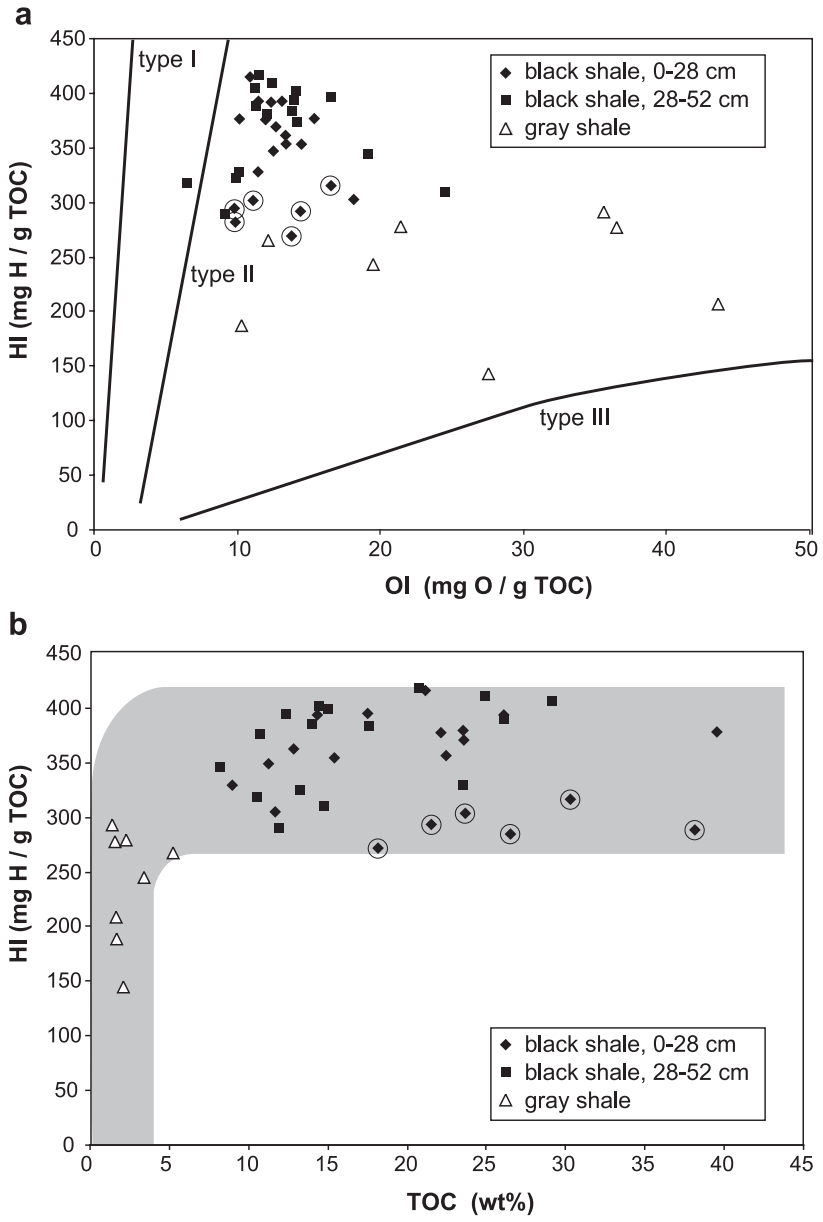

Fig. 5. Rock Eval data. (a) Hydrogen index (HI) vs. oxygen index (OI; "modified van Krevelen plot"). Maturation paths shown for type I–II–III organic matter (e.g., Tyson, 1995). (b) HI vs. TOC; shaded field shows general pattern of covariation. Symbols represent stratigraphic intervals of different redox and organic petrographic character: diamonds=lower black shale (0–28 cm), dominantly organic matter of terrigenous origin; squares=upper black shale (28–52 cm), dominantly organic matter of marine algal origin; triangles=gray shale; circled diamonds are samples from the "illitic zone" at 17–23 cm (see text).

that were deposited hemipelagically and subsequently pyritized.

The first signs of bioturbation in the Hushpuckney Shale are found ~3 cm below the black shale/gray shale contact (Fig. 3). All burrows in the uppermost black shale appear to have been initiated at or above the black shale/gray shale contact and to have penetrated downward from it, consistent with the inference

that benthic conditions were toxic during deposition of the black shale submember. Burrowing intensity was limited below the black shale/gray shale contact (ii2–3), but the overlying gray shale is completely homogenized (ii6) from the contact upward. Discrete burrows and ichnogenera are identifiable in the interval from ~49 to 85 cm (Fig. 3). In stratigraphic succession, the following ichnozones can be identified: (1) ~49–55 cm, large *Trichichnus*, (2) ~55–60 cm, small to medium *Trichichnus*, (3) ~60–70 cm, small to medium *Trichichnus* and *Helminthopsis*, (4) ~70–76 cm, a mixed assemblage dominated by *Zoophycos*, *Phycosiphon* (*Anconichnus*), *Schaubcylindrichnus* (*Terebellina*), and (5) ~76–85 cm, a mixed assemblage dominated by *Planolites* and *Schaubcylindrichnus* (*Terebellina*); *Chondrites* occurs sporadically in the upper zones. These trace fossils are typical of the *Zoophycos* assemblage, which is commonly developed in fine-grained sediments deposited in dysoxic environments (Ekdale and Mason, 1988; Bromley, 1996; Savrda et al., 2001). The basal zones in which only *Trichichnus* is present (~49–60 cm) suggest that benthic O_2 levels remained sufficiently low as to exclude a more diverse trace-fossil assemblage for an extended period after the onset of gray shale sedimentation. Above ~60 cm, substrate type may have been an important influence on benthic tracemakers: *Helminthopsis* generally favors high-porosity "soupground" conditions, whereas the *Zoophycos–Phycosiphon–Schaubcylindrichnus–Planolites* association is typical of somewhat firmer, semiconsolidated substrates (Ekdale et al., 1984; Bromley, 1996).

4.4. Major components

The major components of the study unit are: (1) organic matter, (2) authigenic Fe-sulfide, i.e., pyrite, (3) authigenic phosphate, and (4) siliciclastic minerals, i.e., illite, quartz, mixed-layer I/S, and chlorite (Algeo and Maynard, 1997; Hoffman et al., 1998). These components are effectively proxied by TOC, TS, total phosphorus (TP), and Al_2O_3/SiO_2, respectively (Figs. 4a and 6a–c). The contribution of sulfide S to total S was not determined but is typically ~60–90% in similar facies (cf. Mossmann et al., 1991; Schimmelmann and Kastner, 1993). Most P in the study core (>90%) resides in authigenic phosphate, as shown by (1) strong P–Ca covariation (r^2 0.95; Algeo and Maynard, 1997, p. 99), and (2) a bimodal distribution of total P concentrations with modes at <0.5 wt.% (samples lacking nodules) and >5.0 wt.% (samples containing nodules; unpublished data). The siliciclastic fraction of the study core consists predominantly of detrital illite and quartz, the proportions of which can be proxied by Al_2O_3/SiO_2 ratios (~0 for quartz and ~0.44±0.06 for pure illite, based on chemical analyses in Grim, 1968; Weaver and Pollard, 1973; Newman, 1987). The dominant elemental affinities of the major components, as determined by cluster analysis, are: (1) organic matter: TOC, Ni, Cu, U, Mo, and V; (2) Fe-sulfide: Zn; (3) phosphate: TIC, Ca, P, Sr, Y, and U; and (4) siliciclastics: Si, Zr, Nb, Ti, Mg, Al, K, Rb, Na, Ba, Fe, and Mn (Hoffman et al., 1998, their Fig. 6).

The organic fraction of the study unit consists of four maceral groups: (1) vitrinite, comprising vitridetrinite and desmocollinite; (2) inertinite, comprising inertodetrinite, fusinite, and semifusinite; (3) exinite, comprising mainly alginite; and (4) bituminite (Fig. 4c; cf. Wenger and Baker, 1986). The vitrinitic macerals occur in thin, elongate bands (<1.5×2–80 μm) that are internally structureless and commonly contain embedded grains of clay, pyrite framboids, and inertinite. The inertinitic macerals occur both in association with and independently of vitrinite as thin, elongate bands (<3.5×2–40 μm) or small, very bright, angular grains. Organic matter in the black shale samples exhibited relatively limited variation in hydrogen and oxygen indices (HI and OI), ca. 290–410 mg H g^{-1} TOC and 5–20 mg O g^{-1} TOC, respectively (Fig. 5a; cf. Wenger and Baker, 1986; Hatch and Leventhal, 1992). In contrast, gray shale samples yielded lower and substantially more variable HI and OI values. No relationship exists between TOC and HI for either black shale or gray shale samples, although the latter exhibit systematically lower values for both variables than the former (Fig. 5b). Core black shales of Desmoinesian (Middle Pennsylvanian) age in southeastern Kansas yielded vitrinite reflectance values (R_0) of ~0.3–0.8 (Wenger and Baker, 1986, 1987), so it is unlikely that thermal processes have altered organic matter in the study unit to a significant degree.

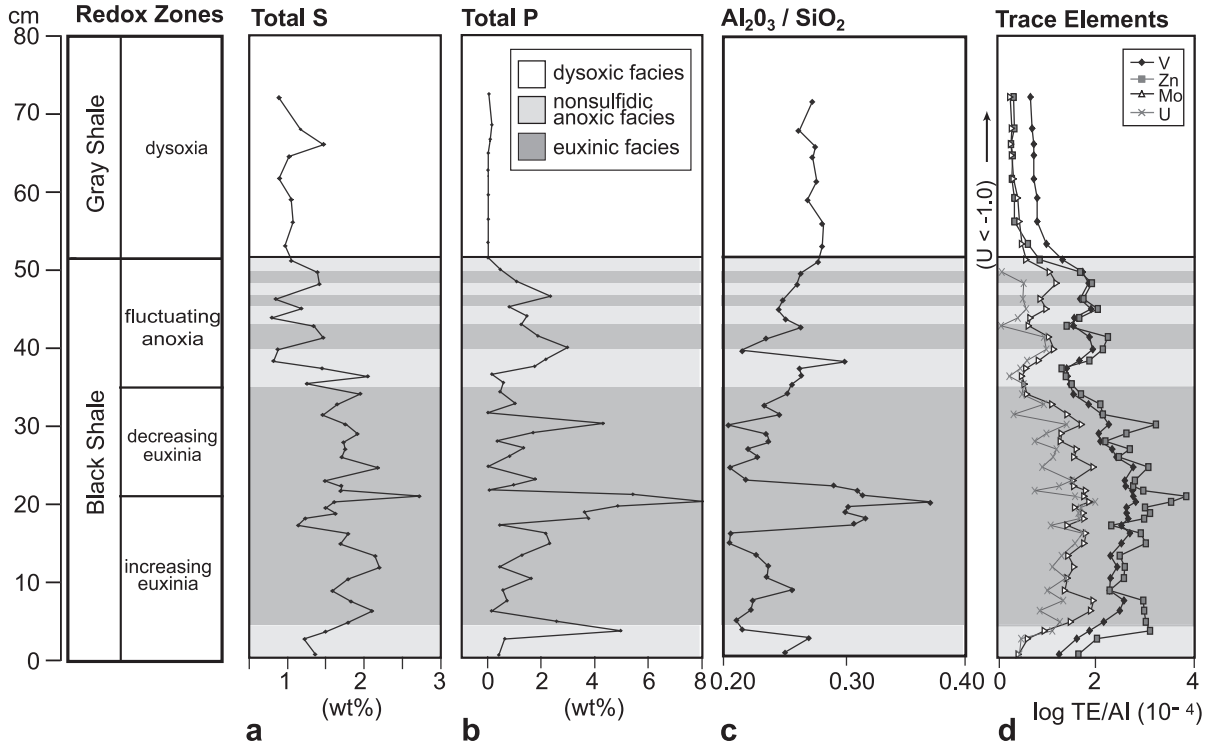

Fig. 6. Major component proxies in the study core. (a) Total S (wt.%), a proxy for authigenic sulfide. (b) Total P (wt.%), a proxy for authigenic phosphate. (c) Al_2O_3/SiO_2, a proxy for detrital siliciclastics. (d) Mo, U, V, and Zn (log TE/Al$\times 10^{-4}$), proxies for paleoredox conditions. Note proxies for the organic fraction of the study core in Fig. 4.

4.5. Stratigraphic trends

4.5.1. Paleoredox proxies

Centimeter-interval sampling allowed detailed analysis of stratigraphic trends in petrographic and geochemical variables within the study unit (Figs. 4 and 6). Because much of the variance of some variables is closely related to paleoredox conditions, stratigraphic trends in redox-sensitive TEs will be considered first. Four TEs (Mo, U, V, and Zn) are enriched in the black shale submember by as much as two to three orders of magnitude over background levels in the gray shale submember (Fig. 6d). These TEs exhibit maximum enrichment factors ($\sim$50–100 for Mo, V, Zn, and $\sim$1000 for U) that are similar to or higher than those from modern euxinic environments (e.g., Jacobs et al., 1987; Brumsack, 1989; Crusius et al., 1996; Dean et al., 1999; Yarincik et al., 2000; Morford et al., 2001) and are thus considered to have "strong euxinic affinity," i.e., a propensity for enrichment under euxinic conditions. Algeo and Maynard (2004) demonstrated that these TEs are useful proxies for paleoredox conditions and developed a procedure based on patterns of TOC–TE covariation for assignment of redox facies (e.g., dysoxic, nonsulfidic anoxic, or euxinic) to individual samples.

These four TEs exhibit very similar patterns of stratigraphic variation (Fig. 6d), a point emphasized by comparison of *Z* scores (Fig. 7a). Based on the redox-facies assignments of Algeo and Maynard (2004), the study unit can be divided into the following redox zones: (1) increasing euxinia (0–21 cm; n.b., nonsulfidic conditions at 0–4 cm), (2) decreasing euxinia (21–35 cm), (3) fluctuating anoxia, with rapid variation between nonsulfidic and sulfidic conditions (35–52 cm), and (4) dysoxia (52–85 cm; shown in Figs. 3–4 and 6–7 as background shading). Noteworthy is the stratigraphic asymmetry of the redox cycle, i.e., the decline in redox potential over a stratigraphic interval of $\sim$21 cm (i.e., from the

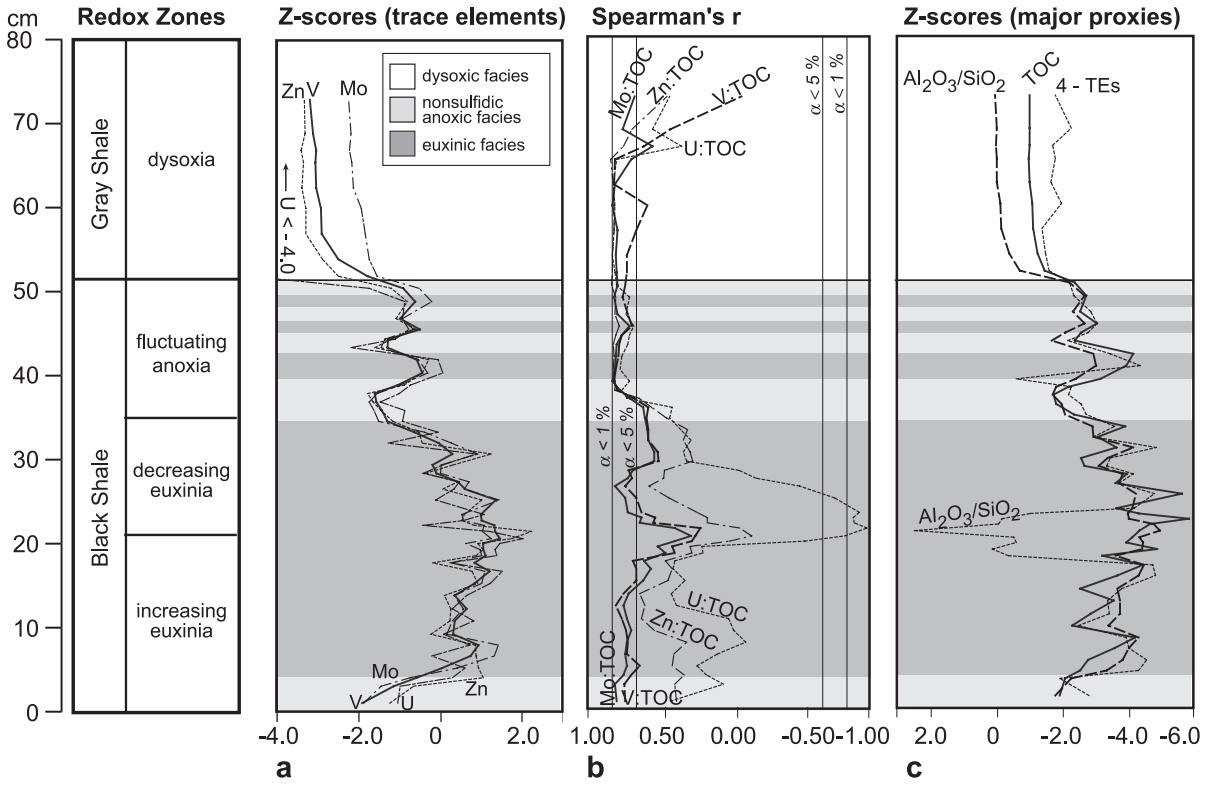

Fig. 7. Statistical analysis of covariation between major component proxies of the study core. (a) *Z* scores for trace-element concentrations (Mo, U, V, Zn; Fig. 5d). *Z* scores represent the normalization of variance in a data set to a mean of 0 and a standard deviation of 1; they are useful in comparing data sets with different ranges of values. (b) Evolutive Spearman's *r* coefficients for TE–TOC pairs. These curves represent correlation coefficients generated in an "evolutive" manner, i.e., calculated using a "sliding window" of seven equally weighted points, and are useful in showing stratigraphic changes in major component relationships. Values approaching 1.00 (toward left) correspond to stronger TE–TOC covariation; 1% and 5% α significance levels are shown as vertical lines. (c) *Z* scores for TOC (Fig. 4a), Al_2O_3/SiO_2 (Fig. 6c), and "4-TEs," i.e., the average *Z* score for the four trace elements in (a). *Z* score calculations were based on variance of black shale samples only (0–52 cm), and *Z* scores for Al_2O_3/SiO_2 in (c) were inverted to better show relationships with TOC and 4-TEs.

transgressive limestone/black shale contact to the mid-lower black shale) and the rise in redox potential over an interval of >60 cm (i.e., from the mid-lower black shale to the top of the gray shale submember; Fig. 8). Also noteworthy are differences in the geochemistry of core intervals deposited under uniformly euxinic (e.g., 4–35 cm) vs. fluctuating anoxic redox conditions (e.g., 35–52 cm): the latter exhibit (1) lower TOC and TS values (Figs. 4a and 6a), and (2) an increase in TOC–TE covariation (r >0.80; Fig. 7b). This last feature is significant because it marks a return to strong coupling between processes of TOC and TE accumulation, suggesting residence of TEs primarily in the organic fraction of the study unit; in contrast, weak TOC–TE covariation in the underlying euxinic zone reflects decoupling of processes of TOC and TE accumulation and residence of TEs primarily in authigenic mineral phases (Algeo and Maynard, 2004).

4.5.2. Organic macerals and Rock Eval data

Petrographic point counts revealed substantial stratigraphic variation in maceral abundances within the study unit (Fig. 4c–d). Vitrinitic and inertinitic macerals are the dominant types from the base of the black shale to ~30 cm, comprising 5–62 vol.% of samples; above ~30 cm, these macerals decline sharply in abundance, comprising <5 vol.% of samples. Exinitic and bituminitic macerals are present in small quantities from the base of the black shale to

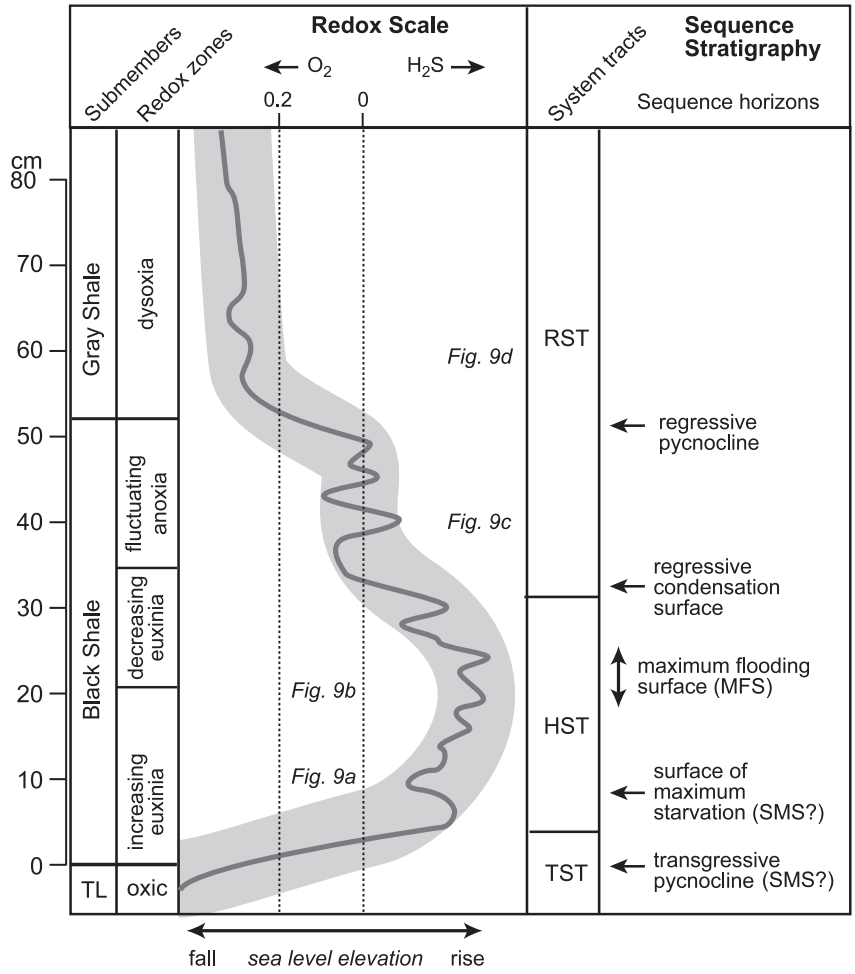

Fig. 8. Paleoredox, eustatic, and sequence stratigraphic features of the study core. Redox potential (dark gray line) is shown relative to a semiquantitative scale; the dysoxic/nonsulfidic anoxic boundary is at 0.2 ml O_2 l^{-1} H_2O, and the nonsulfidic anoxic/euxinic boundary is at 0 ml O_2 l^{-1} H_2O. Sea-level elevation changes (light gray envelope) are inferred to match the "low-order" cycle in redox potential; "high-order" (centimeter-scale) cycles in paleoredox conditions may have been of climatic rather than eustatic origin. Abbreviations: TST=transgressive systems tract, HST=highstand systems tract, RST=regressive systems tract. See text for discussion of sequence horizons.

~30 cm, comprising 0–2 vol.% of samples; above ~30 cm, these macerals increase somewhat in abundance, comprising 2–11 vol.% of samples. Noteworthy is that exinitic and bituminitic macerals are entirely absent in a 6-cm core interval at 17–23 cm (see discussion of "illitic zone" below). The relative dominance of vitrinitic and inertinitic macerals, which are derived from higher land plants, can be expressed by a terrigenous fraction (F_{terr}) that is calculated as the ratio of vitrinite plus inertinite to total organic macerals (Fig. 4d). This variable shows that terrestrially derived macerals are dominant in the lower black shale (F_{terr}=75–100%) but diminish sharply in relative (as well as absolute) abundance above ~30 cm (F_{terr}<50%). An inconsistency between the organic maceral and TOC data deserves comment: total maceral counts decline by a factor of ~10 from the lower (0–30 cm) to the upper (30–52 cm) part of the black shale submember (Fig. 4c), whereas TOC values decline by a factor of only two to three over the same interval (Fig. 4a). This may reflect a systematic undercounting of bituminitic macerals, which are

difficult to identify owing to their diffuse margins and weakly fluorescent character, and which comprise a large proportion of the organic material in the upper part of the black shale submember.

HIs exhibit several patterns of stratigraphic variation in the study core (Fig. 4b). First, the black shale submember yields higher HI values (~290–420) than the overlying gray shale submember (~200–290). Second, within the portion of the black shale submember characterized by numerous redox fluctuations (i.e., 35–52 cm), samples assigned to the nonsulfidic anoxic facies consistently yield lower HI values than adjacent samples assigned to the euxinic facies (~290–330 vs. ~380–420, respectively). Third, within the uniformly euxinic portion of the black shale submember (i.e., 4–35 cm), the 6-cm-thick "illitic zone" at 17–23 cm yields lower HI values than the underlying and overlying core intervals (~270–300 vs. ~350–400, respectively).

4.5.3. Major component proxies

Each of the major component proxies exhibits a characteristic pattern of stratigraphic variation in the study core. The pattern of variation in TOC, a proxy for organic matter, is similar to that in TE concentrations, reflecting a strong link to redox conditions. Within the black shale submember, TOC values rise sharply from ~8 wt.% at the base (0 cm) to a maximum of ~40 wt.% at 20–26 cm, followed by a decline to a minimum of <5 wt.% at 52 cm (i.e., the black shale/gray shale contact; Fig. 4a). Centimeter-scale variation in TOC values is covariant with similar variation in the TE records and, hence, correlates with shifts between nonsulfidic (lower TOC) and euxinic (higher TOC) redox facies. The degree of covariation can be assessed through calculation of "evolutive" Spearman's r coefficients for TOC–TE pairs (Fig. 7b). TOC–TE covariation is (1) moderate for much of the lower and middle black shale interval (0–37 cm), except for the "illitic zone" at 17–23 cm where it is weak; (2) very strong for the upper black and lower gray shale interval (37–65 cm), where r values are mostly >0.80; and (3) generally more pronounced for Mo and V than for Zn or U.

TS, a proxy for authigenic sulfides, exhibits a rather different pattern of stratigraphic variation. In the lower to middle black shale submember (0–37 cm), TS falls within a limited range of values, ~1.6–2.7 wt.% (except for a single outlier). Above 37 cm, there is an abrupt shift to generally lower concentrations, ~1.2–2.0 wt.% (Fig. 6a). The shift to lower TS values occurs not at the black shale/gray shale contact (as with TOC, P, and TEs) but, rather, in the middle of the black shale submember, close to the level at which redox facies change from uniformly euxinic to mixed sulfidic–nonsulfidic character (cf. Cruse and Lyons, 2000, their Fig. 4).

TP, a proxy for authigenic phosphate, exhibits a stratigraphic pattern somewhat similar to TOC and TEs in being enriched in the black shale submember, although there is considerably greater sample-to-sample variation in the TP record (Fig. 6b), which bears little relationship to the TOC and TE records at a centimeter scale. Peaks in the TP record correlate with intervals that have high concentrations of phosphatic granule layers (Fig. 3b).

The proxy for detrital siliciclastics, Al_2O_3/SiO_2, shows a rather complex pattern of stratigraphic variation (Fig. 6c). Al_2O_3/SiO_2 ratios within the black shale submember range from a low of ~0.20 (i.e., a ca. 1:1 mixture of quartz and illite) to a high of ~0.38 (i.e., nearly pure illite, which has a Al_2O_3/SiO_2 ratio of $\sim 0.44 \pm 0.06$). In contrast, Al_2O_3/SiO_2 ratios in the gray shale submember are intermediate and relatively invariant (~0.29–0.31), suggesting a ca. 2:1 mixture of illite and quartz. Most of the black shale is more quartz-rich than the gray shale, although a salient excursion in the middle of the black shale submember (at 17–23 cm) has a distinctly illitic composition (hence, the "illitic zone").

4.5.4. Stratigraphic cyclicity

Owing to strong bioturbation, the gray shale submember of the Hushpuckney–Edmonds core exhibits neither layering nor compositional cyclicity (Figs. 3, 4, and 6). However, the black shale submember exhibits cyclic compositional variation at several stratigraphic scales: (1) a single "low-order" cycle spanning the full 52 cm thickness of the black shale; (2) ~12 "high-order" cycles of 2–7 cm thickness; and (3) millimeter-scale variation. The millimeter-scale variation can be imaged in X-radiographs but is below the level of resolution of petrographic and geochemical data in this study and will not be considered further.

The "low-order" cycle is present in the TOC, TS, TP, and TE records as an excursion from minimum values at the base and top of the black shale to maxima in the middle of the black shale (i.e., at ~20–25 cm; Figs. 4a and 6a,b,d). It is also present in the siliciclastic proxy record, Al_2O_3/SiO_2, which shows high ratios at the base and top of the black shale and a minimum in the middle of the unit (i.e., at ~15–17 and ~23–25 cm, below and above the "illitic zone" at 17–23 cm; Fig. 6c). The presence of a "low-order" cycle in the Al_2O_3/SiO_2 record, similar to those in other major component proxy records, is best demonstrated through a comparison of *Z* scores (Fig. 7c). This clearly reveals the similarities in the Al_2O_3/SiO_2, TOC, and TE records, as well as the distinctly anomalous Al_2O_3/SiO_2 values of the "illitic zone" at 17–23 cm. In some geochemical records, the "low-order" cycle appears to show a minor break at ~35–37 cm, i.e., at the transition from the euxinic redox zone to the fluctuating anoxic redox zone (e.g., Figs. 4a and 8).

"High-order" (i.e., centimeter-scale) cyclicity is present in all geochemical records (Figs. 4 and 6). It is clearly expressed in the TOC record, for example (Fig. 4a), which has 12 or 13, mostly well-defined peaks that exactly match layers of alternately darker (low-density) and lighter (high-density) character in core X-radiographs (Fig. 3a). This correspondence is due to the fact that TOC is the dominant control on X-radiograph gray-scale densities (Algeo and Maynard, 1997). Two characteristics of "high-order" cycles are worth noting: (1) the thicknesses of individual cycles decrease from 4.0–4.5 cm at the base of the black shale (0 cm) to a minimum of 2.0–2.5 cm at ~18–30 cm, and then increase irregularly upward to ~5.0–7.0 cm at the black shale/gray shale contact (52 cm); and (2) the organic-rich hemicycle is relatively thicker for cycles at ~12–37 cm than for those above or below this interval (Fig. 3a; cf. Algeo and Maynard, 1997, p. 136). "High-order" cycles are evident also in the TS, TP, TE, and Al_2O_3/SiO_2 records (Fig. 6), with most peaks correlative with those in the TOC record (e.g., Fig. 7c). An observer might object that many of these "high-order" cycles are defined by three-point trends (i.e., low–high–low) in the geochemical data, raising the issue of whether sample density exceeds the Nyquist frequency (i.e., 2 points per cycle). This would be a concern if the samples were randomly located. However, we chose sample intervals on the basis of X-radiograph gray-scale density patterns, allowing delimitation of centimeter-thick samples of relatively uniform internal character having maximum contrast from adjacent samples. Thus, we are confident that we have "captured" any significant compositional variation that exists at a centimeter scale within the study core.

5. Discussion

5.1. Sedimentation rates and cycle genesis

The black shale submember of core shales is generally considered to have accumulated very slowly under sediment-starved conditions (Heckel, 1977). This is supported by an abundance of phosphatic granule layers in the black shale submember of the study core, many of which show evidence of winnowing and condensation (Fig. 3b). Phosphatic layers typically take hundreds or thousands of years to form in modern marine environments (Föllmi, 1996; Filippelli, 1997), and there are >50 such layers in the study core. Although there is insufficient age control to accurately determine sedimentation rates for the present study unit, general estimates for core shales of Upper Pennsylvanian Kansas-type cyclothems are possible. Long-term average sedimentation rates for Upper Pennsylvanian strata in the Midcontinent range from 5 cm kyr^{-1} cratonward to 20 cm kyr^{-1} basinward (Watney et al., 1991). Thus, a 10- to 20-m-thick cyclothem represents ~50 to 400 kyr, similar to estimates based on average cyclothem duration (Heckel, 1986; Algeo and Wilkinson, 1988; Saller et al., 1994) and on radiometric age dating (Rasbury et al., 1998). Watney et al. (1991) estimated accumulation rates of 1 cm kyr^{-1} for the deepest facies (>50 m water depth, i.e., the core shale) vs. 50–250 cm kyr^{-1} for the regressive shoal-water facies (0–3 m water depth). A similar order-of-magnitude difference in sedimentation rates between deep- and shoal-water facies was determined by gamma analysis of Virgilian–Wolfcampian strata of the East Texas Shelf (Yang and Kominz, 1999). In view of these considerations, we adopt a tentative estimate of 0.5–2.0 cm kyr^{-1} for average sedimentation rates during deposition of the 52-cm-thick black shale submember of

the study core, yielding an estimated duration of ~26–104 kyr.

Compositional cycles in the Hushpuckney Shale may record quasiperiodic climate forcing. Variations in the intensity and seasonality of precipitation were induced by proximity to the paleo-ITCZ, resulting in cyclic long-period climate fluctuations (Fig. 2; Parrish, 1993; Soreghan et al., 2002), and a climatically sensitive, stratified water column was conducive to preserving such fluctuations in the marine record (e.g., Hatch and Leventhal, 1992; Genger and Sethi, 1998; Cruse and Lyons, 2000). Although previous work has implicated Milankovitch-band climate forcing in the genesis of large-scale Midcontinent cyclothems (Heckel, 1986; Yang and Kominz, 1999), the timescales associated with subcyclothemic cycles are largely unknown (e.g., Miller et al., 1996; Miller and West, 1998; Olszewski and Patzkowsky, 2003). Based on an estimated duration of ~26–104 kyr for the Hushpuckney Shale, the ~12 "high-order" cycles of the study core have an average periodicity of ~2 to 9 kyr. These periodicities suggest control by sub-Milankovitch-band (i.e., millennial-scale) climate fluctuations.

5.2. Paleoredox conditions

Determination of benthic O_2 levels in aqueous environments is important for understanding redox-related reactions (e.g., precipitation of authigenic sulfide and oxyhydroxide phases) as well as controls on the preservation and quality of sedimentary organic matter (e.g., Pratt and Davis, 1992; Canfield, 1994; Van Cappellen and Ingall, 1994). Redox conditions in depositional systems are classified as oxic (>~2.0 ml O_2 l^{-1} H_2O), dysoxic or suboxic (~2.0–0.2 ml O_2 l^{-1} H_2O), nonsulfidic anoxic (<~0.2 ml O_2 l^{-1} H_2O, no free H_2S), or euxinic (0 ml O_2 l^{-1} H_2O, with free H_2S; Wignall, 1994). Dysoxic environments are commonly recognized by a depauperate shelly benthos and trace fossils characteristic of low-oxygen conditions (e.g., the *Zoophycos* assemblage; Rhoads et al., 1991; Wignall, 1994). As a practical matter, anoxia is considered to exist whenever dissolved O_2 levels are sufficiently depleted as to exclude all benthic organisms, resulting in a total lack of sediment bioturbation. Analysis of modern environments has shown that such exclusion occurs at a low but positive dissolved oxygen threshold, ca. 0.2 ml O_2 l^{-1} H_2O (e.g., Edwards, 1985; Tyson and Pearson, 1991). Although several special types of redox environments have been recognized, e.g., episodic benthic anoxia (poikiloaerobia; Oschmann, 1991) and stabilization of the oxic/anoxic boundary at the sediment–water interface (exaerobia; Savrda and Bottjer, 1991), the study unit exhibits none of the features associated with them (cf. Wignall, 1994).

In the study core, the black and gray shale submembers of the Hushpuckney Shale are inferred to represent markedly different redox conditions owing to pronounced differences in (1) color and organic carbon content (>2.5 wt.% vs. <2.5 wt.%; Fig. 4a); (2) ichnofabric (laminated vs. bioturbated; Fig. 3a); and (3) concentrations of major component proxies, e.g., total S and P (Fig. 6a–b), and redox-sensitive trace elements (Fig. 6d). With regard to the trace-element data, low and invariant concentrations in the gray shale submember are consistent with residence primarily in the detrital siliciclastic fraction rather than in the organic or sulfidic fractions of the host shale, which is characteristic of oxic to dysoxic marine facies (e.g., Dean et al., 1997, 1999; Adelson et al., 2001). Generally dysoxic conditions are indicated for the gray shale submember of the Hushpuckney–Edmonds core owing to a near-total absence of body fossils and to the presence of a series of low-diversity ichnofossil zones containing ichnogenera commonly associated with low-oxygen conditions (Fig. 3b). Conversely, the laminated character, absence of shelly benthos, and high TE content of the black shale submember (Figs. 3 and 6) are evidence of deposition under conditions of consistently strong oxygen depletion.

The black shale/gray shale contact may record an abrupt rise in benthic dissolved O_2 concentrations (Fig. 8), allowing development of a low-diversity (probably worm-dominated) benthic community and terminating the processes responsible for trace-element enrichment. This is suggested by sharp changes in sediment color, TOC, TE, and TP content, as well as by a marked increase in burrowing intensity. Burrowing of the uppermost ~3 cm of the black shale submember appears to have been initiated entirely at or above the black shale/gray shale contact (Fig. 3), suggesting that bottomwater conditions were unremittingly hostile to benthic colonization below that level. Such a rapid change in paleoredox con-

ditions is most easily explained by lateral migration of the pycnocline in response to eustatic regression (cf. Heckel, 1986; Cruse and Lyons, 2000). Although generally dysoxic conditions prevailed during deposition of the gray shale submember, a succession of ichnofossil zones indicate a progressive increase in benthic O_2 levels. A shift from monospecific occurrences of *Trichichnus* (~49–60 cm) to more diverse ichnofossil associations (~60–85 cm) as well as a transition from a carbonate-free zone of discrete macroburrows (<85 cm) to a calcareous zone of completely homogenized fabric (>85 cm) suggests a progressive rise in benthic O_2 levels. However, the dominant control on ichnofossil occurrences may have been substrate consistency rather than dissolved oxygen. *Helminthopsis* favored "soupground" substrates (60–70 cm), whereas the *Zoophycos–Phycosiphon* (*Anconichnus*)–*Schaubcylindrichnus* (*Terebellina*)–*Planolites* association developed when firmer, semiconsolidated substrates were present (70–85 cm; Fig. 3b; cf. Ekdale et al., 1984).

5.3. Sources of detrital siliciclastics

Regional patterns of variation in siliciclastic proxy records can provide information about the sources and fluxes of detrital material within the Midcontinent Seaway. Based on analysis of three cyclothemic core shales (Hushpuckney, Stark, Muncie Creek) at multiple locales along a ~250-km transect in eastern Kansas, Algeo and Maynard (1997) demonstrated (1) strong linear covariation of Al_2O_3/SiO_2 with K_2O and TiO_2, suggesting a two-component mixing system; and (2) a regional gradient in Al_2O_3/SiO_2 values with higher values to the northeast (their Fig. 7, p. 139). XRD analysis showed that illite and quartz were dominant in all samples, so both siliciclastic fluxes to the Midcontinent Seaway consisted of these two minerals in varying proportions. In the study core, Al_2O_3/SiO_2 values range from a minimum of ~0.20, reflecting a ca. 1:1 mixture of quartz and illite, to a maximum of ~0.38, close to the composition of pure illite (~0.44±0.06; Fig. 6c; Grim, 1968; Weaver and Pollard, 1973; Newman, 1987). The regional gradient in Al_2O_3/SiO_2 values implies derivation of the illite-rich component from the northeast and the quartz-rich component from the southwest. We surmise that the former represents a "cratonic" flux, e.g., detrital material from deep chemical weathering of the craton, although a source in the distal Alleghenian Orogen cannot be excluded, and that the latter represents an "orogenic" flux, e.g., more quartz-rich, and possibly siltier, clastics sourced in the Ouachita–Marathon Orogen or Ancestral Rockies (Fig. 2; cf. Cullers, 1994).

The relationship of detrital siliciclastics to other major components of the study unit provides strong constraints on depositional processes in the Midcontinent Seaway. Similar "low-order" cycles in TOC, TEs, and Al_2O_3/SiO_2 (Fig. 7c) demonstrate that organic carbon accumulation rates, redox conditions, and detrital siliciclastic fluxes must have responded to a common forcing mechanism, either eustasy or a co-related climatic factor. Although changes in TOC concentration and redox conditions might have either eustatic or climatic causes, stratigraphic variation in the siliciclastic proxy provides a strong case for control of the "low-order" cycle by sea-level elevation changes. We reach this conclusion as follows: (1) within the "low-order" cycle, the illite-rich "cratonic" component is dominant at the base and top of the black shale (and in the superjacent gray shale) and the quartz-rich "orogenic" component is dominant in the middle part of the black shale (at ~15–17 and 23–25 cm; excluding the anomalous "illitic zone" at 17–23 cm; Fig. 6c); (2) the "cratonic" flux to the Midcontinent Seaway would have diminished as sea level rose and sediments were sequestered along a paleoshoreline receding hundreds of kilometers to the northeast (Fig. 2); (3) the "orogenic" flux was less responsive to sea-level elevation changes owing to the steeper morphology of the Anadarko Basin to the southwest, minimizing paleoshoreline migrations; hence, sea-level rises resulted in a *relative* increase in the "orogenic" flux; and (4) if climate change were the dominant factor, then more humid interglacial conditions should have enhanced chemical weathering rates and increased the "cratonic" siliciclastic flux, which is contrary to observed Al_2O_3/SiO_2 trends within the "low-order" cycle (note that this scenario might be a viable explanation for the "illitic zone" at 17–23 cm, however). If the siliciclastic proxy record was controlled principally by eustatic rather than climatic changes, then the strongly covariant TOC and TE records (Fig. 7c) must have responded to the same forcing mechanism. Thus, we

infer that the "low-order" cycle in organic carbon accumulation rates, redox conditions, and detrital siliciclastic fluxes were all controlled principally by eustatic changes (Fig. 8). These relationships exist because rising sea-level elevations moved the study site deeper into the oxygen-minimum zone, enhancing benthic O_2 depletion and organic matter preservation, and reducing the flux of the "cratonic" siliciclastic component through sequestering in paralic systems tracts.

The core interval at 17–23 cm, which we termed the "illitic zone," deserves further consideration. Not only does this interval yield the highest Al_2O_3/SiO_2 values in the study unit (0.30–0.38, vs. 0.20–0.28 elsewhere), it is unusual also because (1) its organic fraction consists almost exclusively of vitrinitic and inertinitic macerals (i.e., terrestrially sourced; Fig. 4c), (2) it yields markedly lower HI values than sub- and superjacent core intervals (~270–300 vs. ~350–400; Fig. 4b), and (3) its lower and upper contacts appear to be sharp (e.g., Fig. 6c). The high Al_2O_3/SiO_2 values of this interval suggest a detrital siliciclastic fraction dominated by the "cratonic" component, indeed to a degree shown by no other samples in the study unit, and its sharp contacts suggest sudden shifts between "cratonic" and "orogenic" sources of siliciclastics.

There are several possible interpretations of the "illitic zone." First, it might represent a large but transient eustatic fall that caused an influx of "cratonic" clastics to the Midcontinent. This is unlikely, however, because other geochemical variables (e.g., TOC and TEs) should have responded to a large and rapid change in sea-level elevation, and no such response is observed. Second, the "illitic zone" might represent a transient climatic event of ca. ~3–12 kyr duration (based on average sedimentation rates, Section 5.1), accompanied by little or no change in sea-level elevation. One example of such a climatic event would be an increase in precipitation and runoff into the Appalachian Basin, augmenting the flux of "cratonic" siliciclastics; increased runoff would also lower the salinity of surface waters in adjacent marine areas, thus strengthening the pycnocline and maintaining oxygen-depleted benthic conditions. The "illitic zone" coincides with the interglacial highstand of the Swope cyclothem, and Late Pennsylvanian interglacial stages were generally characterized by higher humidity (Cecil, 1990; Rankey, 1997; West et al., 1997; Soreghan et al., 2002; Olszewski and Patzkowsky, 2003). A third possibility is that the "illitic zone" represents a rafted mat of coal-swamp vegetation that became waterlogged and sank to the seafloor as a unit, which would account for its "cratonic" siliciclastic fraction, abundance of terrestrial-derived organic macerals, and sharp lower and upper contacts. Data of the present study are inadequate to discriminate among the latter two options, but the climatic event hypothesis is favored because the Hushpuckney Shale can be correlated at a centimeter scale between the Edmonds study core and two cores located >100 km to the southwest on the basis of X-radiography (Algeo and Maynard, 1997, p. 136). Correlation of the "illitic zone" and its constituent centimeter-thick layers over such a large area makes the rafted coal mat hypothesis unlikely.

5.4. Sources of organic matter

The proportions of terrestrial- vs. marine-sourced organic matter can be evaluated on the basis of petrographic and Rock Eval data. Petrographic data are useful because vitrinite and inertinite are generally derived from higher terrestrial plant debris, exinite from marine algae, and bituminite from heavily bacterially degraded material usually of marine algal origin (Tyson, 1995). In the study core, much of the vitrinite is woody material that has been gelatinized to varying degrees by bacterial degradation (desmocollinite). The small size and angular character of the inertinite fragments suggest that these may represent charcoal, e.g., burned woody plant tissue. Insight regarding fluxes of terrestrial organics to the Midcontinent Seaway can be gained from a study of penecontemporaneous coal beds of the Western Kentucky Coalfield (Hower et al., 1994). This study showed that wetter intervals were dominated by lycopods and resulted in a relative increase in vitrinite (i.e., peat) production, and that drier intervals were dominated by tree ferns and resulted in a relative increase in inertinite (i.e., charcoal) production. The proportion of inertinite (i.e., I/(I+V)) is significantly lower in these coals (0.15 ± 0.10) than in the black shale submember of the study core (0.24 ± 0.14), indicating preferential transport of charcoal over peat from coastal coal swamps to distal marine shelves,

possibly due to finer particle size and transport via a wind-borne vector.

Rock Eval data may be used to assess organic matter sources, although hydrogen (HI) and oxygen (OI) indices are influenced also by the degree of thermal or bacterial degradation of the organic material. Black shale samples of the study unit exhibit HI and OI values consistent with type II organic matter, generally considered to be of mixed terrestrial–marine origin, whereas the gray shale samples plot between the fields for type II and type III organic matter, the latter either of terrestrial origin or derived from highly altered type II organic matter (Fig. 5a; Tyson, 1995). Alteration of type II organic matter is more likely in the case of gray shale samples of the Hushpuckney–Edmonds core because (1) these samples form a diffuse field contiguous with the type II black shale samples rather than plotting along the type III trendline (Fig. 5a), and (2) petrographic analysis revealed few macerals of terrestrial origin (Fig. 4c). Accepting the Rock Eval data as a provenance indicator implies that organic matter in both the black shale and gray shale submembers of the study unit is of mixed terrigenous–marine derivation. This is at odds with the petrographic data, which show a pronounced shift from terrestrial-dominated to marine-dominated organic matter at ~30 cm (Fig. 4d). The resolution of this inconsistency may be that the Rock Eval data are more reliable as indicators of organic matter quality rather than provenance, although the possibility of undercounting of bituminitic macerals (Section 4.5.2) cannot be fully discounted.

Based on these considerations, we infer that organic matter in the lower to middle black shale (0–30 cm) has a mixed marine–terrestrial source (except for the "illitic zone" at 17–23 cm, in which it is almost entirely of terrestrial origin), and that organic matter in the upper black shale (30–52 cm) and gray shale (52–85 cm) is largely of marine algal origin. We further conclude that organic matter deposited under non-sulfidic anoxic or euxinic redox conditions (i.e., as prevailing during deposition of the black shale submember) underwent little subsequent bacterial degradation, regardless of source, and that organic matter deposited under dysoxic conditions (i.e., as prevailing during deposition of the gray shale submember) was subjected to variable but generally strong bacterial degradation.

The shift from organic macerals of predominantly terrestrial origin to those of predominantly marine origin at ~30 cm (Fig. 4d) is so distinct and unusual as to be worthy of further consideration. We infer that this shift was influenced by both eustatic and climatic factors. If the "low-order" cycle present in most geochemical records was of eustatic origin (see Section 5.3), then maximum highstand conditions were reached at ~20–25 cm within the study core, above which regression commenced (Fig. 8). The shift from transgressive or highstand to regressive systems tracts would have resulted in basinward progradation of paralic facies, filling of estuaries and lagoons, and a reduction in the area of coastal swamps (e.g., Emery and Meyers, 1996; Posamentier and Allen, 1999). As coastal coal swamps were lost, the production and export of terrestrial vegetation was reduced. Climatic change may have played a role in that eustatic regression was the result of renewed growth of southern hemisphere icesheets, which would have been preceded by climatic cooling and an increase in aridity (e.g., Cecil, 1990; West et al., 1997; Soreghan et al., 2002), contributing to the drying out of coastal coal swamps. Increases in the abundances of marine-derived macerals above ~30 cm suggest higher phytoplankton productivity, especially since the higher redox potentials prevailing above ~35 cm would have resulted in poorer preservation of organic matter (Section 4.5.2). Higher primary productivity may be a consequence of climatic rather than eustatic factors. For example, increasing aridity would have reduced runoff around the margins of the Midcontinent Seaway, causing an increase in salinity in the mixed (surfacewater) layer and a weakening of the pycnocline; this, in turn, would have resulted in enhanced upward mixing of nutrients, stimulating primary production.

5.5. Sequence stratigraphy

5.5.1. Stratigraphic horizons in transgressive and highstand systems

Sequence stratigraphers have identified several types of horizons associated with the transgressive to highstand systems tracts of marine sequences. The most important of these are the transgressive surface (TS) and the maximum flooding surface (Van Wagoner et al., 1988). The transgressive surface (TS)

marks the base of the transgressive succession and is characterized by condensed relict sediments deposited in thin shelf blanket or sand shoal geometries; glauconitic sands and phosphorites may be common (Jervey, 1988). Where a lowstand systems tract is absent, the TS merges with the underlying sequence boundary to form an erosion/transgression (E/T) surface (e.g., Olszewski and Patzkowsky, 2003; Brett et al., in press). The MFS marks the top of the transgressive succession and develops at the stratigraphic level at which sediment supply exactly balances subsidence and sea-level rise (Jervey, 1988). It is characterized by a strongly condensed section of thin but laterally extensive hemipelagic or pelagic deposits that may include organic-rich shales (Van Wagoner et al., 1988; Loutit et al., 1988). In a distal marine environment on a stable cratonic shelf (e.g., as in the Late Pennsylvanian Midcontinent Seaway), rates of clastic supply and subsidence are low, so this surface is effectively equivalent to the stratigraphic level at which sea-level elevation was highest and the paleoshoreline transgressed to its most cratonward position. In older literature, the MFS is sometimes referred to as the downlap surface (DLS; e.g., Baum and Vail, 1988; Van Wagoner et al., 1988), a term referring to the geometry of reflection horizons in seismic stratigraphic analysis.

A third horizon, the surface of maximum (sediment) starvation (SMS), was recently proposed by Brett et al. (in press). They considered the SMS to represent the maximum *rate* of sea-level rise, which is conceptually distinct from both the onset of sea-level rise (i.e., the TS) and the maximum sea-level highstand (i.e., the MFS) in a eustatic model based on a smooth sinusoidal curve (e.g., Posamentier and Vail, 1988). According to Brett et al. (in press), SMSs in Upper Ordovician mixed carbonate–clastic successions comprise hardgrounds or corrosion surfaces with pyritic and phosphatic coatings, similar to a TS or MFS, but distinguishable by the deepening facies character of both the underlying and overlying strata. Older literature generally links maximum sediment starvation with the MFS/DLS (n.b., the term "SMS" was originally introduced as a synonym for MFS; Baum et al., 1982; Baum and Vail, 1988), but these studies make clear that condensation can be associated with the entire transgressive systems tract (e.g., Loutit et al., 1988; Van Wagoner et al., 1988). Whether the distinction proposed by Brett et al. (in press) can be widely applied to transgressive successions remains an open question: Irregularities in the pattern of sea-level rise (i.e., nonconformance to the sinusoidal eustatic model) or limited stratigraphic offset between the SMS and MFS might make recognition of the former difficult.

In addition to these sequence-related horizons, stratigraphic successions may record changes in physico-chemical conditions of the water column associated with migration of (1) wave base and (2) the pycnocline. Wave base is typically recognized in marine environments by a change in the quantity of fine-grained sediment; above wave base, near-continuous stirring of seafloor sediments prevents settling of carbonate or siliciclastic mud. Wave base can be quite variable depending on fetch, regional wind patterns, and weather conditions, but approximate depths are 5–15 m for fair-weather conditions, 20–30 m for mid-sized storms, and >200 m for the largest storms (Komar et al., 1972; Nichols, 1999). A pycnocline represents a depth range within which water density changes rapidly, which is a function of the temperature–salinity structure of the water column. Shallow pycnoclines commonly form at the base of the mixed (surfacewater) layer and act as a "floor" on the effects of wave turbulence, whereas deeper pycnoclines develop along permanent thermoclines at depths of ~200–1000 m in modern tropical oceans (Wright and Colling, 1995). Pycnoclines are often associated with oxygen-depleted and, sometimes, sulfidic conditions in the deeper water mass owing to reduced vertical mixing. Modern examples include (1) the Saanich Inlet of British Columbia, where oxygen depletion develops seasonally below a pycnocline at ~60 m with euxinia below ~175–200 m (Jacobs, 1984; Morford et al., 2001); (2) the Cariaco Basin, where oxygen depletion exists below a pycnocline at ~150 m with euxinia below ~300 m (Jacobs, 1984; Lyons et al., 2003); and (3) the Black Sea, where oxygen depletion exists below a pycnocline at ~20–100 m with euxinia below ~100–200 m (Murray et al., 1989; Lyons, 1993; Anderson et al., 1994; n.b., secular variation in the depth of the O_2/H_2S interface has been documented in all of these settings). Lateral migration of either wave base or a pycnocline may leave a stratigraphic record in transgressive and highstand systems tracts.

5.5.2. Stratigraphic horizons in the Hushpuckney Shale

Although the general sequence stratigraphy of Kansas-type cyclothems has been well-studied (e.g., Watney et al., 1989, 1995; Heckel, 1991; Bisnett and Heckel, 1996; Felton and Heckel, 1996), core shales have received little detailed attention in this regard. As shown in this study, however, core black shales contain a number of horizons of distinctive character that may have sequence stratigraphic or environmental significance. In the study core, these include (1) the contact of the black shale submember of the Hushpuckney Shale with the underlying transgressive Middle Creek Limestone (0 cm); (2) an interval at ~8–12 cm marked by a dip in TOC and F_{terr} values (Fig. 4a,d); (3) the "illitic zone" at 17–23 cm, marked by an anomalous Al_2O_3/SiO_2 excursion (Figs. 6c and 7c) as well as by peak values of TOC, vitrinite and inertinite, and TEs (Figs. 4a,c and 6d); (4) the horizon at ~30 cm at which TOC and F_{terr} values decline sharply and exinite and bituminite concentrations increase modestly (Fig. 4a,c,d); (5) the interval at ~28–34 cm containing the greatest density of authigenic phosphatic granule layers and the largest granule sizes (Fig. 3b); (6) the horizon at ~35 cm at which redox conditions shifted from uniformly euxinic to fluctuating sulfidic–nonsulfidic conditions, accompanied by decreases in TOC, HI, TS, and TE values (Figs. 4a,b and 6a,d); and (7) the contact of the black shale submember with the overlying gray shale submember of the Hushpuckney Shale (52 cm; Fig. 3). Our evaluation of these features relies on the preceding discussion of sequence stratigraphic and environmental concepts (Section 5.5.1) and on interpretation of the "low-order" cycle (corresponding to the 52-cm-thick black shale submember of the study unit) as having a eustatic origin (Section 5.3; Fig. 8). Although many of these features might have multiple interpretations when considered in isolation, the range of possible interpretations for each is reduced when considered in the context of the stratigraphic framework of all features.

The MFS represents the point at which sediment supply exactly balances subsidence and sea-level rise, terminating transgression. In a distal marine environment on a stable cratonic shelf (e.g., as in the Midcontinent Seaway), rates of clastic supply and subsidence are very low, so effectively this surface is the point at which the highest eustatic elevation is reached. In the Late Pennsylvanian, eustatic fall would have been due to renewed growth of Gondwanan icesheets, coinciding with or following a change toward cooler climatic conditions. The coeval shift to regressive systems tracts would have resulted in basinward progradation of paralic facies, filling of estuaries, and a reduction in the area of coastal swamps (e.g., Emery and Meyers, 1996; Posamentier and Allen, 1999). These events are reflected in the study core by sharp declines in TOC and F_{terr} at ~30 cm (Fig. 4a,d), so the MFS can be located no higher than this stratigraphic level. If the "low-order" cycle in TOC, TE, and Al_2O_3/SiO_2 values (Fig. 7c) was controlled principally by eustasy (Section 5.3), then the MFS is logically placed at the cycle peak, i.e., at ~17–26 cm (Fig. 8; cf. Heckel, 1977, his Fig. 2). An additional observation supporting this interpretation is that this interval is characterized by the thinnest and most TOC-rich "high-order" (centimeter-scale) cycles in the study core (Fig. 3a; cf. Algeo and Maynard, 1997, p. 136). This suggests that detrital siliciclastic and bulk sedimentation rates were at their lowest at the MFS, a common feature of sea-level highstands.

The surface of maximum (sediment) starvation develops under conditions of maximum rate of sea-level rise and is characterized by (1) strong condensation and (2) the deepening facies character of underlying and overlying strata (Brett et al., in press). It is not clear that a separate surface of this type can be identified in the Hushpuckney–Edmonds core, but one candidate is the contact of the black shale submember with the underlying transgressive limestone (Fig. 8; Carlton Brett, personal communication, 2003). This horizon shows extensive corrosion and microstylolitization although no concentration of pyrite or phosphate, and extensive burrow penetration of the uppermost few cm of the underlying limestone indicates that there was no hardground formation (Section 4.2). As noted earlier, corrosion at this contact may be of post-depositional origin (i.e., associated with downward flux of acidic porefluids from the overlying black shale), so its sequence stratigraphic significance is uncertain. Significantly, "high-order" (centimeter-scale) cycles decrease in thickness and authigenic phosphatic granule layers increase in frequency from the base to the middle of the black

shale (~20–25 cm; Fig. 3), suggesting that sedimentation rates continued to slow during deposition of the lower black shale, which is inconsistent with maximum sediment starvation at the transgressive limestone/black shale contact. As discussed below, we prefer to interpret the transgressive limestone/black shale contact as a record of pycnocline migration. One horizon located above the base of the black shale but below the MFS that shows possible evidence of a slowdown in sedimentation is the core interval at ~8–12 cm, which is characterized by small but measurable decreases in TOC and F_{terr} values (Fig. 4a,d). These decreases might be the consequence of rapid sea-level rise because the organic macerals that dominate the lower black shale are of "detrital" origin (i.e., sourced in coastal coal swamps) and, hence, potentially subject to transgressive sequestering (Fig. 8). However, it is doubtful whether these features are sufficiently diagnostic for designation of the 8–12 cm interval as a "SMS."

One additional horizon in the black shale submember showing evidence of strong condensation has no obvious sequence stratigraphic interpretation. This horizon, located at ~28–34 cm, is characterized by (1) a higher density of authigenic phosphate granule layers, (2) more frequent lens-shaped layers, and (3) larger granule sizes (to 3–4 mm, vs. <1 mm for layers at other levels; Fig. 3b). Further, it is closely associated with the shift from dominantly terrestrial to dominantly marine organic macerals at ~30 cm (Fig. 4d) and with a rapid rise in redox potential, from uniformly euxinic to fluctuating anoxic conditions, at ~30–35 (Fig. 8). Its location above the MFS dictates against an origin through transgressive condensation processes, such as nearshore sequestering of siliciclastics. Rather, it appears to be related to the onset of eustatic regression, an association previously inferred for the changes in organic maceral dominance and paleoredox conditions in the same core interval (Section 5.4). Standard sequence stratigraphic models do not have any mechanism for generating condensed horizons during the early regressive phase, when basinward progradation of nearshore systems tracts causes an increase in sedimentation rates in offshore areas (e.g., Van Wagoner et al., 1988; Jervey, 1988). Such models are based largely on variables controlling the generation and filling of accommodation space (i.e., eustasy, subsidence, and sedimentation), with a secondary role at most assigned to climatic factors. We infer that the condensation horizon at ~28–34 cm is a product of climate changes associated with the early regressive phase of the Swope cyclothem (Fig. 8). Specifically, as climate conditions became more arid with the onset of renewed glaciation and eustatic regression, reduced runoff caused a weakening of the pycnocline in the Midcontinent Seaway, allowing deeper penetration of wave energy and greater stirring of seafloor sediments. A weaker pycnocline also resulted in greater vertical mixing, increasing benthic O_2 levels somewhat and stimulating phytoplankton productivity through upwelling of nutrients (Section 5.4). The onset of regression did not lead to an immediate increase in the flux of clastic sediment to the study site, as predicted by standard sequence stratigraphic models (e.g., Van Wagoner et al., 1988; Jervey, 1988), because of its remoteness from the paleoshoreline (Fig. 2).

The final horizons of potential sequence stratigraphic significance are the lower and upper contacts of the black shale submember of the study unit. Both of these horizons represent abrupt changes in redox potential, i.e., the onset and termination of anoxic conditions (Fig. 8; Sections 4.2 and 5.2). Further, there is a certain symmetry between them in that (1) one is associated with eustatic transgression and the other with eustatic regression, and (2) the black shale samples proximal to both contacts are characterized by similar TOC, TE, and Al_2O_3/SiO_2 values, suggesting similar water mass conditions and sediment fluxes at the onset and termination of the benthic anoxic event (Figs. 4a and 6c,d). These observations are consistent with interpretation of the lower and upper contacts of the black shale submember as a response to lateral migration of the pycnocline across the Midcontinent Shelf, i.e., cratonward during transgression and oceanward during regression. Pycnoclines are often associated with oxygen-depleted deepwater masses in modern marine environments, and, when formed at the base of the mixed layer, are located at water depths slightly greater than wave base (Section 5.5.1). In this case, evidence of wave base might be expected in slightly shallower facies of the Swope cyclothem, i.e., below the transgressive limestone/black shale contact, and above the black shale/gray shale contact. Heckel (1977) proposed that surfaces representing "effective wave base" are present within

the middle (transgressive) and upper (regressive) limestones of some Kansas-type cyclothems, characterized by a shift from grainy oolitic or skeletal carbonates to mudstones or wackestones (transgressive phase) or by the inverse pattern (regressive phase; cf. his Fig. 2). A facies analysis of the transgressive Middle Creek and regressive Bethany Falls limestones of the Swope Formation is beyond the scope of the present study, but internal facies transitions of this type are indeed present (Schutter, 1983; Heckel, 1988), consistent with lateral migration of wave base in conjunction with sea-level changes of the Swope glacio-eustatic cycle.

5.6. Climato-environmental dynamics of the Late Pennsylvanian Midcontinent Seaway

General environmental models for the Midcontinent Seaway have been developed in earlier studies (Heckel, 1977, 1991; Hatch and Leventhal, 1992; Hoffman et al., 1998; Genger and Sethi, 1998). These models have some important features in common, e.g., a strong proximal halocline, maintained by freshwater runoff into the Appalachian Basin and easterly trade winds, and a weaker distal thermocline, characterized by less intense benthic anoxia (cf. Algeo and Maynard, 1997). However, existing environmental models for the Midcontinent Seaway are based to only a limited degree on an analysis of the temporal dynamics of the system, e.g., as reflected by the internal sequence and event stratigraphy of core shales. The high-resolution stratigraphic framework of the present study allows development of a dynamic climato-environmental model for the late transgressive to early regressive phases of glacio-eustatic cycles of the Late Pennsylvanian Midcontinent Seaway (Fig. 9). This model integrates eustatic, climatic, and environmental factors to account for the various features of the study core within their proper stratigraphic context (Fig. 8).

The end of the Late Pennsylvanian glacial stage associated with the Hertha/Swope sequence boundary (Fig. 1a) resulted in a major eustatic transgression, recorded in the Middle Creek Limestone and the lowermost ~20 cm of the Hushpuckney Shale (Fig. 8). Deepening of the Midcontinent Seaway caused cratonward migration of wave base and the pycnocline, the successive passage of which was recorded by a lithofacies transition within the Middle Creek Limestone and by the contact of the limestone with the overlying Hushpuckney Shale (Fig. 9a). Owing to oxygen depletion of the water mass below the pycnocline, deposition of organic-rich sediments commenced with passage of the pycnocline across the study site (0 cm, i.e., base of black shale). As the rate of sea-level rise approached its maximum (~8–12 cm), the flux of terrestrial organic matter from coastal coal swamps may have been reduced slightly owing to nearshore sediment sequestering, producing a "surface of maximum starvation". Sea-level elevations reached a highstand during the ensuing interglacial stage (~17–25 cm), which was marked by enhanced climatic humidity (cf. Cecil, 1990; West et al., 1997; Soreghan et al., 2002) and significant increases in the flux of terrestrial organics and illite-rich "cratonic" siliciclastics to the Midcontinent Seaway (Fig. 9b). Coastal coal swamps reached their maximum development at this stage, leading to the export of large quantities of vitrinite (peat) and inertinite (charcoal). High levels of precipitation and runoff around the margins of the Midcontinent Seaway caused a strengthening of the pycnocline, resulting in maximum depletion of benthic O_2 and development of sulfidic conditions in the deepwater mass.

With the onset of renewed Gondwanan icesheet growth, sea-level fall commenced and climatic conditions became cooler and more arid (Fig. 9c; cf. Cecil, 1990; West et al., 1997; Soreghan et al., 2002). Climatic drying caused a loss of coastal coal swamps, a process reinforced by basinward retreat of the shoreline (cf. Emery and Meyers, 1996; Posamentier and Allen, 1999). Climatic drying also reduced runoff into the Midcontinent Seaway, causing the low-salinity surfacewater lens to recede shoreward at a rate exceeding the basinward advance of the paleoshoreline. Both the loss of paralic coal swamps and decreased runoff into the Midcontinent Seaway contributed to a reduction in the flux of terrestrial organic matter to open marine areas. Shoreward retreat of the low-salinity surfacewater lens had the further effect of weakening the pycnocline, resulting in fluctuating benthic redox conditions, an increase in marine productivity owing to enhanced upward mixing of nutrient-rich deepwaters into the photic zone, and greater reworking of bottom sediments and generation of phosphate gran-

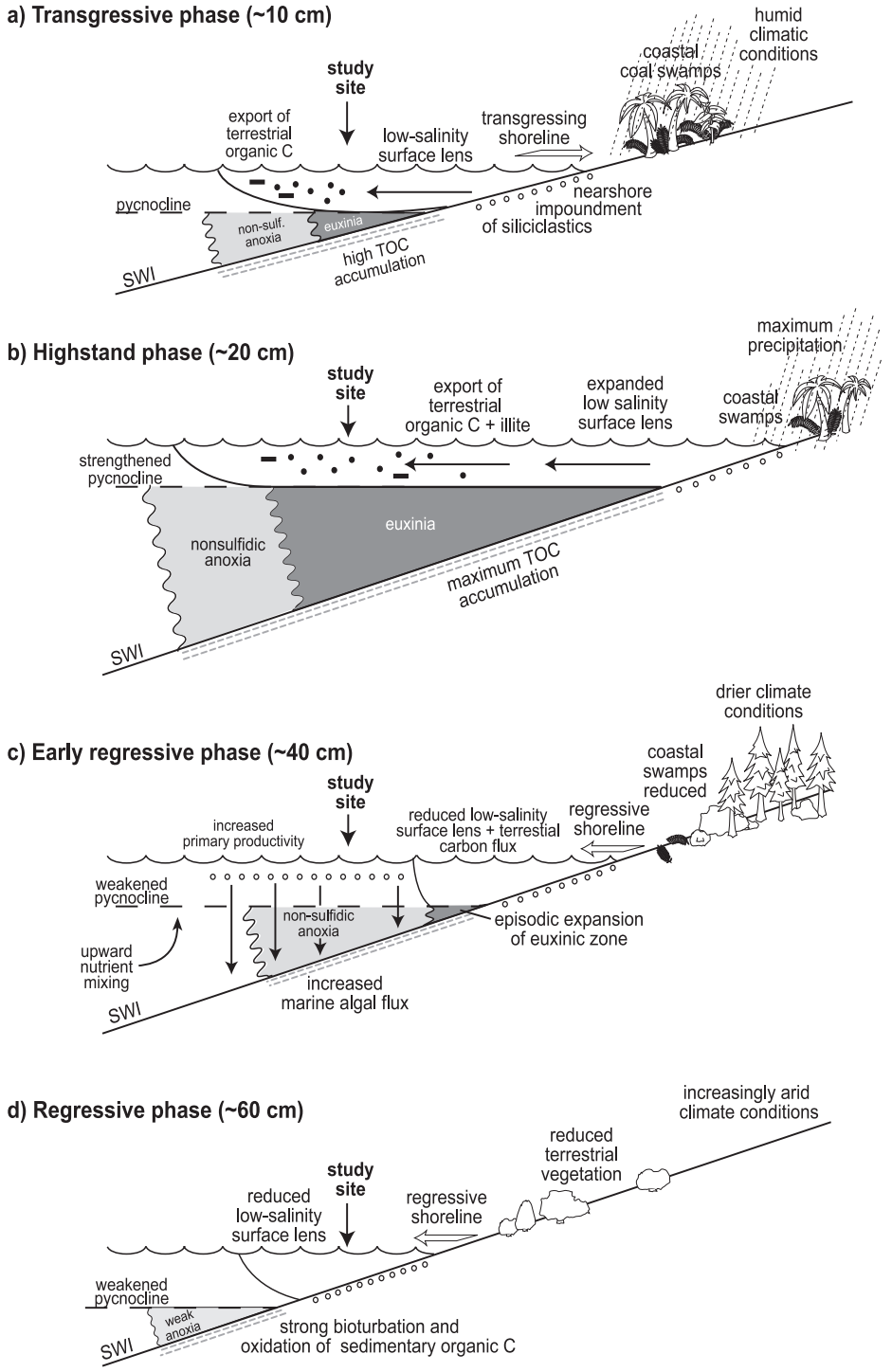

Fig. 9. Model of evolving climato-environmental system of the Late Pennsylvanian Midcontinent Seaway. Panels (a) through (d) represent conditions at 10, 20, 40, and 60 cm above the base of the black shale submember of the study core and are keyed to the sea-level curve in Fig. 8. See text for discussion.

ule layers owing to deeper penetration of wave energy. Continued eustatic fall resulted in an increase in the flux of siliciclastics across the shelf owing to fluvial incision of emergent upper shelf areas, and, eventually, to migration of the pycnocline basinward across the study site, resulting in an abrupt transition to dysoxic conditions on the seafloor (Fig. 9d; cf. Cruse and Lyons, 2000).

6. Conclusions

(1) The Hushpuckney Shale records the late transgressive to early regressive phases of a Gondwanan Ice Age glacio-eustatic cycle. It represents an archive of high-frequency compositional variation, allowing reconstruction of climato-environmental dynamics within the penecontemporaneous Midcontinent Seaway.

(2) Paleoredox conditions ranged from dysoxic to strongly euxinic during deposition of the study unit. The 52-cm-thick black shale submember of the study unit was deposited under anoxic conditions, with redox potential declining from the base of the black shale (0 cm) to a minimum at ~21 cm. Uniformly euxinic conditions persisted from ~4 to 35 cm, above which fluctuating sulfidic–nonsulfidic conditions existed to the black shale/gray shale contact at 52 cm. The overlying ~36-cm-thick gray shale submember of the study unit was deposited under uniformly dysoxic conditions.

(3) The black shale exhibits no bioturbation except in its uppermost ~3 cm, which was penetrated by burrows initiated at or above the contact with the overlying gray shale. The transition to dysoxic conditions in the gray shale allowed establishment of a benthic community of soft-bodied organisms that increased in abundance and diversity as dissolved oxygen levels increased upsection. This resulted in a series of discrete ichnozones in the gray shale dominated by (1) large *Trichichnus*, (2) small–medium *Trichichnus*, (3) *Helminthopsis–Trichichnus*, and (4) *Zoophycos–Phycosiphon–Schaubcylindrichnus–Planolites*. Substrate consistency was a secondary factor, with soupgrounds preferred by the *Helminthopsis–Trichichnus* association and firmgrounds by the *Zoophycos–Phycosiphon–Schaubcylindrichnus–Planolites* association.

(4) Covariation among organic carbon accumulation rates, paleoredox conditions, and detrital siliciclastic fluxes, as proxied by TOC, trace-element concentrations, and Al_2O_3/SiO_2, reflects common forcing mechanisms. A single "low-order" cycle, comprising the full 52-cm thickness of the black shale submember and representing ~26–104 kyr, was the product of glacio-eustatic transgression/regression. Within this submember, ~12 "high-order" cycles of 2 to 7 cm thickness may be a record of high-frequency (~2–9 kyr) climatic variation, e.g., in precipitation and runoff.

(5) Within the black shale submember, a number of horizons may have sequence stratigraphic or environmental significance. The base and top of the black shale are interpreted as a record of lateral migration of the pycnocline during sea-level transgression and regression, and the MFS, marking the eustatic highstand, is present at ~17–25 cm in the middle of the black shale submember. A "SMS" within the transgressive succession below the MFS cannot be identified beyond doubt, but a "regressive condensation surface" is present above the MFS, at ~28–34 cm.

(6) The maximum flooding surface at ~17–25 cm is associated with a large excursion toward higher Al_2O_3/SiO_2 values (illitic zone), maximum TOC values, dominance of terrestrial-derived organic macerals (i.e., vitrinite and inertinite), a decrease in HI values, and peak concentrations of redox-sensitive trace elements. These features may reflect more humid interglacial climatic conditions, such that an increase in precipitation and runoff around the margins of the Midcontinent Seaway enhanced the flux of illite-rich "cratonic" siliciclastics and the export of coal-swamp vegetation, while a simultaneous strengthening of the pycnocline resulted in maximum benthic O_2 depletion and, possibly, reduced upwelling of nutrients and marine algal productivity.

(7) The "regressive condensation surface" at ~28–34 cm contains a high density of authigenic

phosphate granule layers and maximum granule sizes and is closely associated with an increase in the absolute abundance of exinite and bituminite, a shift in dominance from terrestrial- to marine-derived macerals (at ~30 cm), and a rapid rise in redox potential from strongly euxinic to fluctuating sulfidic–nonsulfidic conditions (at ~30–35 cm). These features may reflect increased aridity associated with renewed Gondwanan icesheet growth and the onset of eustatic regression, e.g., climatic drying and shoreline progradation destroyed coastal coal swamps and reduced the flux of terrestrial-derived organic macerals, and reduced precipitation and runoff into the Midcontinent Seaway weakened the pycnocline, allowing deeper penetration of wave energy, greater winnowing of seafloor sediments, and enhanced upwelling of nutrient-rich deep-waters, stimulating marine algal productivity.

Acknowledgements

Thanks to W. Lynn Watney (Kansas Geological Survey) for loan of the study cores, to Mary Droser (University of California at Riverside) for assistance with identification of ichnogenera, to Erika Elswick (Indiana University) for Leco analyses, to Phil Heckel (University of Iowa) for helpful discussions, to Rich Schultz (Elmhurst College) and Sue Rimmer (University of Kentucky) for editorial handling of the manuscript, to Ariel Anbar (University of Rochester), Joe Hatch (U.S.G.S.), and Carl Brett (University of Cincinnati) for constructive reviews, and to Evelyn Mohalski-Pence (University of Cincinnati) for drafting services. A portion of the geochemical data was taken from MSc theses completed at the University of Cincinnati by David Hoffman and Mikhail Cherny. **[LW]**

References

Adelson, J.M., Helz, G.R., Miller, C.V., 2001. Reconstructing the rise of recent coastal anoxia; molybdenum in Chesapeake Bay sediments. Geochim. Cosmochim. Acta 65, 237–252.

Algeo, T.J., Maynard, J.B., 1997. Cyclic Sedimentation of Appalachian Devonian and Midcontinent Pennsylvanian Black Shales: Analysis of Ancient Anoxic Marine Systems—A Combined Core and Field Workshop: Joint Meeting of Eastern Section AAPG and The Society for Organic Petrography (TSOP), Lexington, Kentucky, Sept. 27–28. Department of Geology, University of Cincinnati, Cincinnati, Ohio. 147 pp. (homepages.uc.edu/~algeot/homepage/publications.htm).

Algeo, T.J., Maynard, J.B., 2004. Trace-element behavior and redox facies in core shales of Upper Pennsylvanian Kansas-type cyclothems. Chem. Geol., 206, 289–318 (this issue).

Algeo, T.J., Wilkinson, B.H., 1988. Periodicity of mesoscale Phanerozoic sedimentary cycles and the role of Milankovitch orbital modulation. J. Geol. 96, 313–322.

Algeo, T.J., Phillips, M., Jaminski, J., Fenwick, M., 1994. High-resolution X-radiography of laminated sediment cores. J. Sediment. Petrol. A64, 665–668.

Anderson, R.F., Lyons, T.W., Cowie, G.L., 1994. Sedimentary record of a shoaling of the oxic/anoxic interface in the Black Sea. Mar. Geol. 116, 373–384.

Arbenz, J.K., 1989. The Ouachita system. In: Bally, A.W., Palmer, A.R. (Eds.), The Geology of North America—An Overview (v. A). Geol. Soc. Am., Boulder, Colorado, pp. 371–396.

Arthur, M.A., Jenkyns, H.C., Brumsack, H.J., Schlanger, S.O., 1990. Stratigraphy, geochemistry, and paleoceanography of organic carbon-rich Cretaceous sequences. In: Ginsburg, R.N., Beaudoin, B. (Eds.), Cretaceous Resources, Events and Rhythms. Kluwer Academic Publishing, Amsterdam, pp. 75–119.

Baum, G.R., Vail, P.R., 1988. Sequence stratigraphic concepts applied to Paleogene outcrops, Gulf and Atlantic basins. In: Wilgus, C.K., Hastings, B.S., Posamentier, H., Van Wagoner, J., Ross, C.A., Kendall, C.G. (Eds.), Sea-Level Changes: An Integrated Approach. Spec. Publ.-Soc. Econ. Paleontol. Mineral., vol. 42, pp. 309–327.

Baum, G.R., Vail, P.R., Hardenbol, J., 1982. Unconformities and depositional sequences in relation to eustatic sea level change, Gulf and Atlantic Coastal Plains. Interregional Geological Correlation Program, Project, vol. 174. Baton Rouge, Louisiana. 3 pp.

Bisnett, A.J., Heckel, P.H., 1996. Sequence stratigraphy helps to distinguish offshore from nearshore black shales in the Midcontinent Pennsylvanian succession. In: Witzke, B.J., Ludvigson, G.A., Day, J. (Eds.), Paleozoic Sequence Stratigraphy: Views from the North American Craton. Spec. Pap.-Geol. Soc. Am., vol. 306, pp. 341–350.

Boardman, D.R., Heckel, P.H., 1989. Glacial–eustatic sea-level curve for early Late Pennsylvanian sequence in north-central Texas and biostratigraphic correlation with curve for midcontinent North America. Geology 17, 802–805.

Bordenave, M.L., Espitalié, J., Leplat, P., Oudin, J.L., Vandenbroucke, M., 1993. Screening techniques for source rock evaluation. In: Bordenave, M.L. (Ed.), Applied Petroleum Geochemistry. Éditions Technip, Paris, pp. 219–278.

Brett, C.B., McLaughlin, P.I., Baird, G.C., Cornell, S.R., in press. Comparative sequence stratigraphy of two classic Upper Ordovician successions, Trenton Shelf (New York–Ontario) and Lexington Platform (Kentucky–Ohio): implications for eustasy and local tectonism in eastern Laurentia. Palaeogeog. Palaeoclimat. Palaeoecol.

Bromley, R.G., 1996. Trace Fossils—Biology, Taphonomy and Applications, 2nd ed. Chapman & Hall, London. 361 pp.

Brumsack, H.J., 1989. Geochemistry of recent TOC-rich sediments from the Gulf of California and the Black Sea. Geol. Rundsch. 78, 851–882.

Canfield, D.E., 1994. Factors influencing organic carbon preservation in marine sediments. Chem. Geol. 114, 315–329.

Cecil, C.B., 1990. Paleoclimate controls on stratigraphic repetition of chemical and siliciclastic rocks. Geology 18, 533–536.

Connolly, W.M., Stanton Jr., R.J., 1992. Interbasinal cyclostratigraphic correlation of Milankovitch band transgressive–regressive cycles: correlation of Desmoinesian–Missourian strata between southeastern Arizona and the midcontinent of North America. Geology 20, 999–1002.

Coveney Jr., R.M., Shaffer, N.R., 1988. Sulfur-isotope variations in Pennsylvanian shales of the midwestern United States. Geology 16, 18–21.

Crowell, J.C., 1978. Gondwanan glaciation, cyclothems, continental positioning, and climate change. Am. J. Sci. 278, 1345–1372.

Crowell, J.C., 1999. Pre-Mesozoic Ice ages: their bearing on understanding the climate system. Geol. Soc. Am., Mem. 192 (106 pp.).

Crowley, T.J., Baum, S.K., 1991. Estimating Carboniferous sea-level fluctuations from Gondwanan ice extent. Geology 19, 975–977.

Crowley, T.J., Hyde, W.T., Short, D.A., 1989. Seasonal cycle variations on the supercontinent of Pangaea. Geology 17, 457–460.

Crowley, T.J., Yip, K.-J., Baum, S.K., Moore, S.B., 1996. Modeling Carboniferous coal formation. Paleoclimates 2, 159–177.

Cruse, A.M., Lyons, T.W., 2000. Sedimentology and geochemistry of the Hushpuckney and Upper Tackett shales: cyclothem models revisited. Geol. Surv. Circ. (Oklahoma) 103, 185–194.

Crusius, J., Calvert, S., Pedersen, T., Sage, D., 1996. Rhenium and molybdenum enrichments in sediments as indicators of oxic, suboxic and sulfidic conditions of deposition. Earth Planet. Sci. Lett. 145, 65–78.

Cullers, R.L., 1994. The controls on the major and trace element variation of shales, siltstones, and sandstones of Pennsylvanian–Permian age from uplifted continental blocks in Colorado to platform sediment in Kansas, USA. Geochim. Cosmochim. Acta 58, 4955–4972.

Dean, W.E., Gardner, J.V., Piper, D.Z., 1997. Inorganic geochemical indicators of glacial–interglacial changes in productivity and anoxia of the California continental margin. Geochim. Cosmochim. Acta 61, 4507–4518.

Dean, W.E., Piper, D.Z., Peterson, L.C., 1999. Molybdenum accumulation in Cariaco basin sediment over the past 24 k.y.: a record of water-column anoxia and climate. Geology 27, 507–510.

Droser, M.L., Bottjer, D.J., 1993. Trends and patterns of Phanerozoic ichnofabrics. Annu. Rev. Earth Planet. Sci. 21, 205–225.

Edwards, B.D., 1985. Bioturbation in a dysaerobic, bathyal basin: California borderland. In: Curran, H.A. (Ed.), Biogenic Structures: Their Use in Interpreting Depositional Environments. Spec. Publ.-Soc. Econ. Paleontol. Mineral., vol. 35, pp. 309–331.

Ekdale, A.A., Mason, T.R., 1988. Characteristic trace–fossil associations in oxygen-poor sedimentary environments. Geology 16, 720–723.

Ekdale, A.A., Muller, L.N., Novak, M.T., 1984. Quantitative ichnology of modern pelagic deposits in the abyssal Atlantic. Palaeogeog. Palaeoclimat. Palaeoecol. 45, 189–223.

Emery, D., Meyers, K.J., 1996. Sequence Stratigraphy. Blackwell, Oxford. 297 pp.

Espitalié, J., La Porte, J.L., Madec, M., Marquis, F., Le Plat, P., Paulet, J., Boutefeu, A., 1977. Méthode rapide de caractérisation des roches mères de leur potentiel pétrolier et de leur degré d'évolution. Rev. Inst. Fr. Pét. 32, 23–42.

Espitalié, J., Deroo, G., Marquis, F., 1985. Rock Eval pyrolysis and its applications. Revue de ÍInstitut Francais du Pétrole Part I, 40, 653–578; Part II, 40, 755–784; Part III, 41, 73–89.

Ettensohn, F.R., 1992. Changing interpretations of Kentucky geology: layer cake, facies, flexure, and eustasy. Misc. Rep.-Geol. Surv. Ohio 5 (184 pp.).

Falcon, R.M.S., Snyman, C.P., 1986. An Introduction to Coal Petrography: Atlas of Petrographic Constituents in the Bituminous Coals of Southern Africa. Rev. Pap.-Geol. Soc. S. Afr., vol. 2.

Felton, R.M., Heckel, P.H., 1996. Small-scale cycles in Winterset Limestone Member (Dennis Formation, Pennsylvanian of northern Midcontinent) represent 'phased regression'. In: Witzke, B.J., Ludvigson, G.A., Day, J. (Eds.), Paleozoic Sequence Stratigraphy: Views from the North American Craton. Spec. Pap.-Geol. Soc. Am., vol. 306, pp. 389–397.

Filippelli, G.M., 1997. Controls on phosphorus concentration and accumulation in oceanic sediments. Mar. Geol. 139, 231–240.

Föllmi, K.B., 1996. The phosphorus cycle, phosphogenesis and marine phosphate-rich deposits. Earth-Sci. Rev. 40, 55–124.

Frakes, L.A., Francis, J.E., Syktus, J.I., 1994. Climate Modes of the Phanerozoic. Cambridge Univ. Press, Cambridge. 274 pp.

Genger, D., Sethi, P., 1998. A geochemical and sedimentological investigation of high-resolution environmental changes within the Late Pennsylvanian (Missourian) Eudora core black shale of the Mid-Continent region, USA. In: Schieber, J., Zimmerle, W., Sethi, P.S. (Eds.), Shales and Mudstones, vol. 1. Schweizerbart'sche, Stuttgart, pp. 271–293.

Grim, R.E., 1968. Clay Mineralogy, 2nd ed. McGraw-Hill, New York. 596 pp.

Hatch, J.R., Leventhal, J.S., 1992. Relationship between inferred redox potential of the depositional environment and geochemistry of the Upper Pennsylvanian (Missourian) Stark Shale Member of the Dennis Limestone, Wabaunsee County, Kansas, USA. Chem. Geol. 99, 65–82.

Heckel, P.H., 1977. Origin of phosphatic black shale facies in Pennsylvanian cyclothems of mid-contintent North America. Am. Assoc. Pet. Geol. Bull. 61, 1045–1068.

Heckel, P.H., 1986. Sea-level curve for Pennsylvanian eustatic marine transgressive–regressive depositional cycles along midcontinent outcrop belt, North America. Geology 14, 330–334.

Heckel, P.H., 1988. Classic "Kansas" cyclothems. In: Hayward, O.T. (Ed.), South-Central Section of the Geological Society of America. Centennial Field Guide, vol. 4. Geological Society of America, Boulder, Colorado, pp. 43–56.

Heckel, P.H., 1991. Thin widespread Pennsylvanian black shales of

Midcontintent North America: a record of a cyclic succession of widespread pycnoclines in a fluctuating epeiric sea. In: Tyson, R.V., Pearson, T.H. (Eds.), Modern and Ancient Continental Shelf AnoxiaSpec. Publ.-Geol. Soc. Lond., vol. 58, pp. 259–273.

Heckel, P.H., 1994. Evaluation of evidence for glacial–eustatic control over marine Pennsylvanian cyclothems in North America and consideration of possible tectonic effects. In: Dennison, J.M., Ettensohn, F.R. (Eds.), Tectonic and Eustatic Controls on Sedimentary Cycles. SEPM Concepts in Sedimentology and Paleontology, vol. 4, pp. 65–87.

Hoffman, D.L., Algeo, T.J., Maynard, J.B., Joachimski, M.M., Hower, J.C., Jaminski, J., 1998. Regional and stratigraphic variation in bottomwater anoxia in offshore core shales of Upper Pennsylvanian cyclothems from the Eastern Midcontinent Shelf (Kansas), USA. In: Schieber, J., Zimmerle, W., Sethi, P.S. (Eds.), Shales and Mudstones, vol. 1. Schweizerbart'sche, Stuttgart, pp. 243–269.

Hower, J.C., Helfrich, C.T., Williams, D.A., 1994. Palynologic and petrographic intervals in the upper Pennsylvanian McLeansboro Group, western Kentucky. Int. J. Coal Geol. 26, 117–132.

Hutton, A.C., 1987. Petrographic classification of oil shales. Int. J. Coal Geol. 8, 203–231.

Jacobs, L.A., 1984. Metal Geochemistry in Anoxic Marine Basins. PhD dissertation, U. of Washington. 217 pp.

Jacobs, L., Emerson, S., Huested, S.S., 1987. Trace metal geochemistry in the Cariaco Trench. Deep Sea Res. A34, 965–981.

Jervey, M.T., 1988. Quantitative geological modeling of siliciclastic rock sequences and their seismic expression. In: Wilgus, C.K., Hastings, B.S., Posamentier, H., Van Wagoner, J., Ross, C.A., Kendall, C.G. (Eds.), Sea-Level Changes: An Integrated Approach, vol. 42. Spec. Publ.-Soc. Econ. Paleontol. Mineral., Tulsa, Oklahoma, pp. 47–69.

Joeckel, R.M., 1994. Virgilian (Upper Pennsylvanian) paleosols in the Upper Lawrence Formation (Douglas Group) and in the Snyderville Shale Member (Oread Formation, Shawnee Group) of the northern Midcontinent, USA: pedologic contrasts in a cyclothem sequence. J. Sediment. Res. 64A, 853–866.

Joeckel, R.M., 1999. Paleosol in Galesburg Formation (Kansas City Group, Upper Pennsylvanian), northern Midcontinent, USA: evidence for climate change and mechanisms of marine transgression. J. Sediment. Res. 69, 720–737.

Kidder, D.L., Hussein, R.A.M., Mapes, R.H., Eddy-Dilek, C.A., 1996. Regional diagenetic variation in maximum-transgression phosphates from Midcontinent Pennsylvanian shales. In: Witzke, B.J., Ludvigson, G.A., Day, J. (Eds.), Paleozoic Sequence Stratigraphy: Views from the North American Craton. Spec. Pap.-Geol. Soc. Am., vol. 306, pp. 351–358.

Komar, P.D., Neudeck, R.H., Kulm, L.D., 1972. Observations and significance of deep water oscillatory ripple marks on the Oregon continental shelf. In: Swift, P.J.P., Duane, D.B., Pilkey, O.H. (Eds.), Shelf Sediment Transport: Process and Pattern. Dowden, Hutchinson and Ross, Stroudsberg, Pennsylvania, pp. 601–619.

Loutit, T.S., Hardenbol, J., Vail, P.R., Baum, G.R., 1988. Condensed sections: the key to age determination and correlation of continental margin sequences. In: Wilgus, C.K., Hastings, B.S., Posamentier, H., Van Wagoner, J., Ross, C.A., Kendall, C.G. (Eds.), Sea-Level Changes: An Integrated Approach. Spec. Publ.-Soc. Econ. Paleontol. Mineral., vol. 42, pp. 183–213.

Lyons, T.W., 1993. Evidence for large pre-industrial perturbations of the Black Sea chemocline. Nature 365, 538–540.

Lyons, T.W., Werne, J.P., Hollander, D.J., Murray, R.W., 2003. Contrasting sulfur geochemistry and Fe/Al and Mo/Al ratios across the last oxic-to-anoxic transition in the Cariaco Basin, Venezuela. Chem. Geol. 195, 131–157.

Mazzullo, S.J., 1998. Stratigraphic architecture of Lower Permian, cyclic carbonate reservoirs (Chase Group) in the Mid-Continent U.S.A., based on outcrop studies. Am. Assoc. Pet. Geol. Bull. 82, 464–483.

Miller, K.B., West, R.R., 1998. Identification of sequence boundaries within cyclic strata of the Lower Permian of Kansas, USA: problems and alternatives. J. Geol. 106, 119–132.

Miller, K.B., McCahon, T.J., West, R.R., 1996. Lower Permian (Wolfcampian) paleosol-bearing cycles of the US Midcontinent: evidence of climatic cyclicity. J. Sediment. Res. 66, 71–84.

Morford, J.L., Russell, A.D., Emerson, S., 2001. Trace metal evidence for changes in the redox environment associated with the transition from terrigenous clay to diatomaceous sediment, Saanlich Inlet, BC. Mar. Geol. 174, 355–369.

Mossmann, J.-R., Aplin, A.C., Coleman, M.L., Curtis, C.D., 1991. Geochemistry of inorganic and organic sulphur in organic-rich sediments from the Peru margin. Geochim. Cosmochim. Acta 55, 3581–3595.

Murray, J.W., Jannasch, H.W., Honjo, S., Anderson, R.F., Reeburgh, W.S., Top, Z., Friedrich, G.E., Codispoti, L.A., Izdar, E., 1989. Unexpected changes in the oxic/anoxic interface in the Black Sea. Nature 338, 411–413.

Newman, A.C.D., 1987. Chemistry of Clays and Clay Minerals. Mineralogical Society Monograph, vol. 6. Wiley, New York. 480 pp.

Nichols, G., 1999. Sedimentology and Stratigraphy. Blackwell, Oxford. 355 pp.

Olszewski, T.D., Patzkowsky, M.E., 2003. From cyclothems to sequences: the record of eustasy and climate on an icehouse epeiric platform (Pennsylvanian–Permian, North American Midcontinent). J. Sediment. Res. 73, 15–30.

Oschmann, W., 1991. Anaerobic–poikiloaerobic–aerobic: a new facies zonation for modern and ancient neritic redox facies. In: Einsele, G., Ricken, W., Seilacher, A. (Eds.), Cycles and Events in Stratigraphy. Springer, Berlin, pp. 565–571.

Parrish, J.T., 1993. Climate of the supercontinent Pangea. J. Geol. 101, 215–233.

Posamentier, H.W., Allen, G.P., 1999. Siliciclastic Sequence Stratigraphy; Concepts and Applications. Soc. Sediment Geol. (SEPM-SSG) Concepts Sedimentol. Paleontol., vol. 7. 210 pp.

Posamentier, H.W., Vail, P.R., 1988. Eustatic controls on clastic deposition II—sequence and systems tracts models. In: Wilgus, C.K., Hastings, B.S., Posamentier, H., Van Wagoner, J., Ross, C.A., Kendall, C.G. (Eds.), Sea-Level Changes: An Integrated ApproachSpec. Publ.-Soc. Econ. Paleontol. Mineral., vol. 42, pp. 125–154.

Pratt, L.M., Davis, C.L., 1992. Intertwined fates of metals, sulfur, and organic carbon in black shales. In: Pratt, L.M., Comer, J.B., Brassell, S.C. (Eds.), Geochemistry of Organic Matter in Sediments and Sedimentary Rocks. SEPM Short Course Notes, vol. 27, pp. 1–27.

Rankey, E.C., 1997. Relations between relative changes in sea level and climate shifts: Pennsylvanian–Permian mixed carbonate–siliciclastic strata, western United States. Geol. Soc. Amer. Bull. 109, 1089–1100.

Rasbury, E.T., Hanson, G.N., Meyers, W.J., Holt, W.E., Goldstein, R.H., Saller, A.H., 1998. U–Pb dates of paleosols: constraints on late Paleozoic cycle durations and boundary ages. Geology 26, 403–406.

Rhoads, D.C., Mulslow, S.G., Gutschik, R., Baldwin, C.T., Stolz, J.F., 1991. The dysaerobic zone revisited: a magnetic facies? In: Tyson, R.V., Pearson, T.H. (Eds.), Modern and Ancient Continental Shelf Anoxia. Spec. Publ.-Geol. Soc. Lond., vol. 58, pp. 187–199.

Ross, C.A., Ross, J.R.P., 1985. Late Paleozoic depositional sequences are synchronous and worldwide. Geology 13, 194–197.

Saller, A.H., Dickson, J.A.D., Boyd, S.A., 1994. Cycle stratigraphy and porosity in Pennsylvanian and Lower Permian shelf limestones, eastern Central Basin Platform, Texas. Am. Assoc. Pet. Geol. Bull. 78, 1820–1842.

Saltzman, M.R., 2003. Late Paleozoic ice age: oceanic gateway or pCO2? Geology 31, 151–154.

Savrda, C.E., Bottjer, D.J., 1991. Oxygen-related biofacies in marine strata: an overview and update. In: Tyson, R.V., Pearson, T.H. (Eds.), Modern and Ancient Continental Shelf Anoxia. Spec. Publ.-Geol. Soc. Lond., vol. 58, pp. 201–219.

Savrda, C.E., Browning, J.V., Krawinkel, H., Hesselbo, S.P., 2001. Firmground ichnofabrics in deep-water sequence stratigraphy. Tertiary clinoform-toe deposits, New Jersey slope. Palaios 6, 294–305.

Schimmelmann, A., Kastner, M., 1993. Evolutionary changes over the last 1000 years of reduced sulfur phases and organic carbon in varved sediments of the Santa Barbara Basin, California. Geochim. Cosmochim. Acta 57, 67–78.

Schultz, R.B., Coveney Jr., R.M., 1992. Time-dependent changes for Midcontinent Pennsylvanian black shales. Chem. Geol. 99, 83–100.

Schutter, S., 1983. Petrology, Clay Mineralogy, Paleontology, and Depositional Environments of Four Missourian (Upper Pennsylvanian) Shales of Midcontinent and Illinois Basins. PhD dissertation, U. of Iowa. 1208 pp.

Schutter, S., Heckel, P.H., 1985. Missourian (early Late Pennsylvanian) climate in Midcontinent North America. Int. J. Coal Geol. 5, 111–140.

Scotese, C.R., 1994. Carboniferous paleocontinental reconstructions. U.S. Geol. Surv. Bull. 2110, 3–6.

Soreghan, G.S., Giles, K.A., 1999. Amplitudes of Late Pennsylvanian glacioeustasy. Geology 27, 255–258.

Soreghan, G.S., Elmore, R.D., Lewchuk, M.T., 2002. Sedimentologic–magnetic record of western Pangean climate in upper Paleozoic loessite (lower Cutler beds, Utah). Geol. Soc. Amer. Bull. 114, 1019–1035.

Tyson, R.V., 1995. Sedimentary Organic Matter. Chapman & Hall, London. 615 pp.

Tyson, R.V., Pearson, T.H., 1991. Modern and ancient continental shelf anoxia: an overview. In: Tyson, R.V., Pearson, T.H. (Eds.), Modern and Ancient Continental Shelf Anoxia. Spec. Publ.-Geol. Soc., vol. 58, pp. 1–26.

Van Cappellen, P., Ingall, E.D., 1994. Benthic phosphorus regeneration, net primary production, and ocean anoxia: a model of the coupled marine biogeochemical cycles of carbon and phosphorus. Paleoceanography 9, 677–692.

Van Wagoner, J.C., Posamentier, H.W., Mitchum, R.M., Vail, P.R., Sarg, J.F., Loutit, T.S., Hardenbol, J., 1988. An overview of the fundamentals of sequence stratigraphy and key definitions. In: Wilgus, C.K., Hastings, B.S., Posamentier, H., Van Wagoner, J., Ross, C.A., Kendall, C.G. (Eds.), Sea-Level Changes: An Integrated Approach. Spec. Publ.-Soc. Econ. Paleontol. Mineral., vol. 42, pp. 39–45.

Veevers, J.J., Powell, C.M., 1987. Late Paleozoic glacial episodes in Gondwanaland reflected in transgressive–regressive depositional sequences in Euramerica. Geol. Soc. Amer. Bull. 98, 475–487.

Watney, W.L., French, J.A., Franseen, E.K., 1989. Sequence stratigraphic interpretations and modeling of cyclothems in the Upper Pennsylvanian (Missourian) Lansing, and Kansas City groups in eastern Kansas. Kansas Geol. Soc., Lawrence, Kansas, 41st Annual Fieldtrip Guidebook. 211 pp.

Watney, W.L., Wong, J.-C., French Jr., J.A., 1991. Computer simulation of Upper Pennsylvanian (Missourian) carbonate-dominated cycles in western Kansas. In: Franseen, E.K., Watney, W.L., Kendall, C.G. (Eds.), Sedimentary Modeling: Computer Simulations and Methods for Improved Parameter Definition. Geol. Surv. Bull., Kansas, vol. 233, pp. 415–430.

Watney, W.L., French, J.A., Doveton, J.H., Youle, J.C., Guy, W.J., 1995. Cycle hierarchy and genetic stratigraphy of Middle and Upper Pennsylvanian strata in the Upper Midcontinent. In: Hyne, N.J. (Ed.), Sequence Stratigraphy of the Mid-Continent. Spec. Publ.-Geol. Soc. Tulsa, vol. 4, pp. 141–192.

Weaver, C.E., Pollard, L.D., 1973. The Chemistry of Clay Minerals. Developments in Sedimentology, vol. 15. Elsevier, New York. 213 p.

Wenger, L.M., Baker, D.R., 1986. Variations in organic geochemistry of anoxic–oxic black shale–carbonate sequences in the Pennsylvanian of the Midcontinent, USA. Org. Geochem. 10, 85–92.

Wenger, L.M., Baker, D.R., 1987. Variations in vitrinite reflectance with organic facies—examples from Pennsylvanian cyclothems of the Midcontinent, USA. Org. Geochem. 11, 411–416.

West, R.R., Archer, A.W., Miller, K.B., 1997. The role of climate in stratigraphic patterns exhibited by late Palaeozoic rocks exposed in Kansas. Palaeogeog. Palaeoclimat. Palaeoecol. 128, 1–16.

Wignall, P.B., 1994. Black Shales. Clarendon Press, Oxford. 127 pp.

Wright, J., Colling, A., 1995. Seawater: Its Composition, Properties and Behaviour. The Open University, Milton Keynes, England. 168 pp.

Yang, W., Kominz, M.A., 1999. Testing periodicity of depositional

cyclicity, Cisco Group (Virgilian and Wolfcampian), Texas. J. Sediment. Res. 69, 1209–1231.

Yarincik, K.M., Murray, R.W., Lyons, T.W., Peterson, L.C., Haug, G.H., 2000. Oxygenation history of bottom waters in the Cariaco Basin, Venezuela, over the past 578,000 years: results from redox-sensitive metals (Mo, V, Mn, and Fe). Paleoceanography 15, 593–604.

Youle, J.C., Watney, W.L., Lambert, L.L., 1994. Stratal hierarchy and sequence stratigraphy—Middle Pennsylvanian, southwestern Kansas, USA. In: Klein, G.D. (Ed.), Pangea: Paleoclimate, Tectonics, and Sedimentation During Accretion, Zenith, and Breakup of a Supercontinent. Spec. Pap.-Geol. Soc. Am., vol. 288, pp. 267–285.